

Results of a Search for γ Dor and δ Sct Stars with the *Kepler* spacecraft

P.A. Bradley

XCP-6, MS F-699 Los Alamos National Laboratory, Los Alamos, NM 87545

pbradley@lanl.gov

J.A. Guzik

XTD-NTA, MS T-086 Los Alamos National Laboratory, Los Alamos, NM 87545

L.F. Miles

XCP-6, MS F-699 Los Alamos National Laboratory, Los Alamos, NM 87545

K. Uytterhoeven

Instituto de Astrofísica de Canarias, 38200 La Laguna, Tenerife, Spain and Departamento de Astrofísica, Universidad de La Laguna, 38200 La Laguna, Tenerife, Spain

J. Jackiewicz

New Mexico State University, Las Cruces, NM 88003

and

K. Kinemuchi

Apache Point Observatory, Sunspot, NM 88349

ABSTRACT

The light curves of 2768 stars with effective temperatures and surface gravities placing them near the gamma Doradus/delta Scuti instability region were observed as part of the Kepler Guest Observer program from Cycles 1 through 5. The light curves were analyzed in a uniform manner to search for gamma Doradus, delta Scuti, and hybrid star pulsations. The gamma Doradus, delta Scuti, and hybrid star pulsations extend asteroseismology to stars slightly more massive (1.4 to 2.5 M_{\odot}) than our Sun. We find 207 gamma Doradus, 84 delta Scuti, and 32 hybrid candidate stars. Many of these stars are cooler than the red edge of the gamma Doradus instability strip as determined from ground-based observations made before *Kepler*. A few of our gamma Doradus candidate stars lie on the hot side of the ground-based gamma Doradus instability strip. The hybrid candidate stars cover the entire region between 6200 K and the blue edge of the ground-based delta Scuti instability strip. None of our candidate stars are hotter than

the hot edge of the ground-based delta Scuti instability strip. Our discoveries, coupled with the work of others, shows that *Kepler* has discovered over 2000 gamma Doradus, delta Scuti, and hybrid star candidates in the 116 square degree *Kepler* field of view. We found relatively few variable stars fainter than magnitude 15, which may be because they are far enough away to lie between spiral arms in our Galaxy, where there would be fewer stars.

Subject headings: Space vehicles:instruments — Stars:rotation — Stars: variable:delta Scuti — Stars:variable:general

1. Introduction

The *Kepler* spacecraft (Borucki 2010; Koch et al. 2010) was launched on 2009 March 6 with the primary goal of searching for extrasolar planet transits. However, the micromagnitude precision of the *Kepler* light curves make *Kepler* observations ideal for finding new pulsating variable stars. Two classes of variable stars with spectral types A and F are of particular interest to us. These are the gamma Doradus (γ Dor) and delta Scuti (δ Sct) stars. They are slightly more massive (1.4 to 2.5 solar masses) and slightly hotter (effective temperature $T_{\text{eff}} = 6500$ to 8500 K) than our Sun. The known γ Dor stars pulsate with periods from 0.3 to 3 days and the gravity modes (g modes) are driven by the convective blocking mechanism (Guzik et al. 2000; Dupret 2004; Grigahcène et al. 2005). They are generally cooler than δ Sct stars, with a T_{eff} between 6500 and 7500 K. δ Sct star pulsations are low-order pressure modes (p modes) and mixed character modes (displaying p mode and g mode properties) driven by the kappa, gamma mechanism acting in the He II ionization region. Their periods range from 30 minutes to 5 hours, and the T_{eff} values are typically between 7000 and 8000 K. The overlap of T_{eff} and surface gravity ($\log g$) ranges for these two types of variables suggests the possibility that some stars might show both γ Dor and δ Sct (so-called hybrid) pulsation behavior. This hybrid behavior is especially exciting for asteroseismology, since the g modes of γ Dor stars sample deeper regions of the star than the p modes and mixed modes (with p and g mode properties) of δ Sct stars. Ground-based observations discovered only four (Henry & Feckel 2005; Uytterhoeven et al. 2008; Handler 2009) hybrid stars. The gamma Doradus (γ Dor), delta Scuti (δ Sct) and “hybrid” stars span the transition between lower mass stars with radiative cores, relatively deep convective envelopes, and solar-like oscillations (like the Sun) and higher mass stars that have convective cores and radiative envelopes (such as β Cephei and slowly pulsating B stars). Current pulsation theory (Guzik et al. 2000; Dupret et al. 2004) shows that there is a complicated energy flow regulation by the convection zone and helium partial ionization zones that determines what type of pulsation mode a given γ Dor, δ Sct, or hybrid star can pulsate in. Grigahcène et al. (2010) and Uytterhoeven et al. (2011) found from *Kepler* data many more hybrid star candidates and that they occupy a broader region of the T_{eff} , $\log g$ space than current stellar pulsation theory predicts. This means that our understanding is incomplete on the structure of the outer layers (δ Sct star pulsations probe this region) and the deeper layers

between the convective core and outer convection zone (γ Dor star pulsations probe this region). Alternatively, our understanding of the driving mechanisms of these stars is incomplete.

However, γ Dor-type pulsations are hard to observe from the ground due to the relatively low amplitude and approximately one day period of the pulsations. Space-borne telescopes do not suffer these limitations and the MOST satellite discovered two bright hybrid candidates (King et al. 2006; Rowe et al. 2006). The larger telescope of the COROT satellite revealed more candidate hybrid stars (Hareter et al. 2010). As mentioned above, the initial data sample from the *Kepler* spacecraft (Grigahcène et al. 2010) revealed that many of the δ Sct and γ Dor stars found were in fact, hybrid star candidates. However, some of the low frequency modes may possibly be Nyquist reflections of high frequency modes (Murphy et al. 2013). Uytterhoeven et al. (2011) followed up by studying a large (> 750 star) sample of γ Dor/ δ Sct candidates that had been labelled as γ Dor or δ Sct candidates by the *Kepler* Asteroseismic Science Operations Center (KASOC). Of the 471 stars that exhibited δ Sct or γ Dor pulsations, 36% (171 stars) were hybrid star candidates. The *Kepler* spacecraft also discovered many non-hybrid γ Dor and δ Sct star candidates. Balona et al. (2011) examined over 10,000 *Kepler* stars for γ Dor pulsations. They found 137 stars with asymmetric light curves (characterized by strong beating and one or two dominant peaks in the Fourier Transform (FT)). Another 1035 stars were approximately symmetric with respect to their maxima and minima, and finally there were 108 stars with many peaks of relatively low amplitude. Some of the stars that have periods consistent with γ Dor variability have temperatures that lie outside the known instability strip. Many of these stars possibly have rotating starspots instead, but spectroscopic data would be needed to confirm this. Tkachenko et al. (2013) screened the publicly available quarter 0 through quarter 8 data, along with their Guest Observer data to search for γ Dor variability and supplemented this with spectroscopic data to confirm their identification as γ Dor pulsators and locate them more accurately in an H–R diagram. Balona and Dziembowski (2011) examined over 12,000 *Kepler* stars for δ Sct variability and found 1568 δ Sct candidate stars. They found that the maximum amplitude distribution increases towards smaller amplitudes. That is, many more δ Sct stars have their largest modes below 100 ppm rather than above 1000 ppm. They also found that no more than 50% of the stars within the δ Sct temperature range were variable, which implies that temperature alone is not the deciding factor for δ Sct pulsations, and that other factors, such as evolutionary state or surface gravity may also play a role in δ Sct variability.

In summary, the previous satellite surveys show several things. First, γ Dor candidates are relatively numerous. The relatively small number of *bona fide* γ Dor stars discovered with ground based observations was the result of selection effects due to their small amplitudes and their periods being near 1 day. Periods near 1 day are very difficult to discern from the ground due to aliasing and transparency variations. Second, hybrid stars are common. Finally, the large number of modes seen in some stars (Poretti et al. 2009; Garcia et al. 2009; Chapellier 2011) shows that higher ℓ modes are present at low amplitudes. We collected Guest Observer data from quarters 1 through 17 of a large sample of previously unobserved stars that were mostly fainter than magnitude 14.

Our goal was to discover candidate γ Dor, δ Sct, and hybrid stars and determine their T_{eff} and $\log g$ distribution. We examined stars that were within and cooler than the ground based instability strip. In particular, we wanted to answer several questions. First, do the new candidate stars lie within the previously established ground-based instability strip boundaries? Second, what is the magnitude limit of *Kepler*'s ability to detect variable star candidates? Finally, what is the relative frequency of γ Dor, δ Sct, and hybrid stars at faint magnitudes and how does it compare to other observations involving brighter stars and/or previously known candidates?

The rest of the paper is organized as follows. We describe our *Kepler* dataset in more detail in Section 2. Section 3 provides an overview of our frequency analysis. We discuss the frequency spectra of our target stars in Section 4 and we summarize our findings in Section 5.

2. Data

The *Kepler* spacecraft monitors the brightness variations of about 150,000 stars in a 10^5 square degree field between Cygnus and Lyra. Brown et al. (2011) obtained multi-band photometry (griz, DD051, and JHK from the Two Micron All Sky Survey) for more than 4 million stars in the *Kepler* field. With these colors, T_{eff} , $\log g$, visual absorption (A_v), metallicity, and radius were derived. About 150,000 of these stars were selected for continuous monitoring by the *Kepler* spacecraft. The observations were obtained with a single filter whose effective wavelength is close to that of the Johnson R filter (Koch et al. 2010). The magnitudes from this bandpass are referred to as *Kepler* magnitudes (K_p) in the *Kepler* Input Catalog (KIC). The light curves were obtained in short cadence (1 minute (Gilliland 2010)) or long cadence (30 minutes (Jenkins et al. 2010)). Each quarter, the stars monitored can change as the *Kepler* planet search team refines their target selection and new objects are added by participants in the *Kepler* Guest Observer program. All *Kepler* stars are given a unique identification (KIC number), which we use in this paper.

In our study, we select stars whose KIC parameters imply a location in or near the δ Sct and γ Dor instability strips, that is, late A to mid F spectral types. Our Guest Observer (GO) sample was limited on the bright side by all the stars brighter than 14.0 being reserved for observations by others (especially the planet transit mission). The faintness limit and contamination factor were set to keep the number of stars requested at a manageable level (a few thousand). The effective temperature range is $8200 > T_{\text{eff}} > 6200$ K, and the $\log g$ range is 3.8 to 4.5. We chose a wider range of T_{eff} and $\log g$ than has been seen in the ground-based instability strip to account for the ± 250 K effective temperature and ± 0.25 dex $\log g$ measurement uncertainties (Molenda-Zakowicz et al. 2011; Uytterhoeven et al. 2011). We also wanted to ensure that we considered stars outside the ground-based instability strip, especially on the cool side in order to confirm that the red edge of the instability strip is not the result of ground-based sensitivity limits. Our selection criteria, coupled with the brighter stars ($<$ magnitude 14) near 8000 K being observed by others, resulted in relatively few stars in our sample near the δ Sct blue edge, as shown in Figure 1. As a result, we expect a significant fraction of our stars will be nonvariable, because they lie outside the ground-

based instability strip, which we initially assume to apply to the space-based data.

In the end, we observed 2768 stars with *Kepler* as part of the GO program. Pinsonneault et al. (2012) showed that the KIC temperatures are actually about 200 K higher than believed, and we applied this shift to select the star sample in Cycle 4 (Quarter 13-Quarter 17). Our sample stars are shown in Figure 1, along with the ground-based instability strips. The stars of Cycle 2 and 3 were selected based on limiting magnitude ($\text{mag} < 15.5$) and contamination factor cutoff ($< 10^{-3}$ for Cycle 2 and $< 10^{-2}$ for Cycle 3). The stars from Cycle 4 had a higher contamination factor limit (< 0.05) and in addition showed variability in sequences of full-frame images taken in Cycle 0 (Kinemuchi et al. 2011). With few exceptions, we chose no stars brighter than magnitude $K_p < 14.0$ or fainter than 16.0 (the few exceptions will be discussed separately). Almost all of the stars lie between $K_p = 14.0$ and 15.5 (see Figure 2 for a magnitude distribution). The T_{eff} and $\log g$ values were mostly derived from photometry for all of our program stars, and hence the observational error bars are relatively large (± 250 K and ± 0.25 dex for T_{eff} and $\log g$, respectively) (Molenda-Zakowicz et al. 2011; Uytterhoeven et al. 2011).

In addition to the Cycle 2 through 4 data, we obtained Cycle 1 observations of 14 stars that were known to be variables or have T_{eff} and $\log g$ consistent with γ Dor or δ Sct pulsations. Nine of these stars were selected to lie within the ground-based hybrid temperature range of 6900 K to 7350 K and have magnitudes between 14 and 15, while the other five stars were variables selected from the All-Sky Automated Survey (ASAS; Pigulski et al. (2010)) and had color indices consistent with being a δ Sct or γ Dor star. The δ Sct, γ Dor, hybrid, and eclipsing binary stars from this 14 star sample will be counted towards the total number of stars, but they will not be included in our discussion of the instability strip location.

The majority of the observations were made in long cadence (~ 30 minute integrations per observation), although some early (Quarter 2 and 4) observations were made in short-cadence mode (~ 1 minute integrations per observation). The bias towards long cadence data in our observations may affect our ability to determine the periods of δ Sct stars with frequencies above the Nyquist limit. However, the observations of 14 stars in Quarters 2 and 4 (Cycle 1) in both long and short cadence mode demonstrated that the δ Sct stars were easily detectable in long cadence mode (see also Balona and Dziembowski 2011). Also, Murphy et al. (2013) show that it is possible to determine the correct super-Nyquist frequencies from long-cadence *Kepler* data. Once we determine that a star shows variability, the delta Scuti nature can be confirmed.

3. Frequency Analysis

We analyzed the data from the 2768 stars in a consistent manner. The data were taken from the Mikulski Archive for Space Telescopes (MAST)¹ database and we analyzed the PDCSAP_FLUX

¹For more information see <http://archive.stsci.edu/kepler>

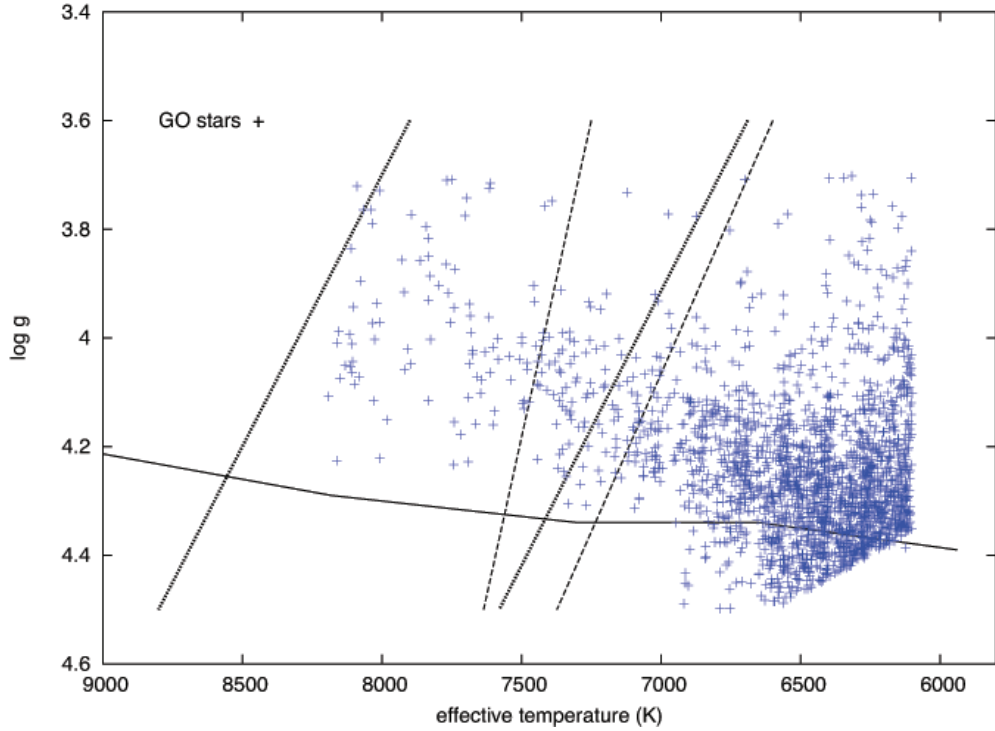


Fig. 1.— Location of our sample stars shifted by +200 K (labeled GO) in the T_{eff} , $\log g$ diagram. The ground-based δ Sct (thick dotted lines; Rodriguez and Breger 2001) and γ Dor (thin dashed lines; Handler and Shobbrook 2002) instability strips are indicated, along with the zero-age main sequence (solid line; Cox 2000). Note that relatively few stars lie within the ground-based δ Sct and γ Dor instability strips.

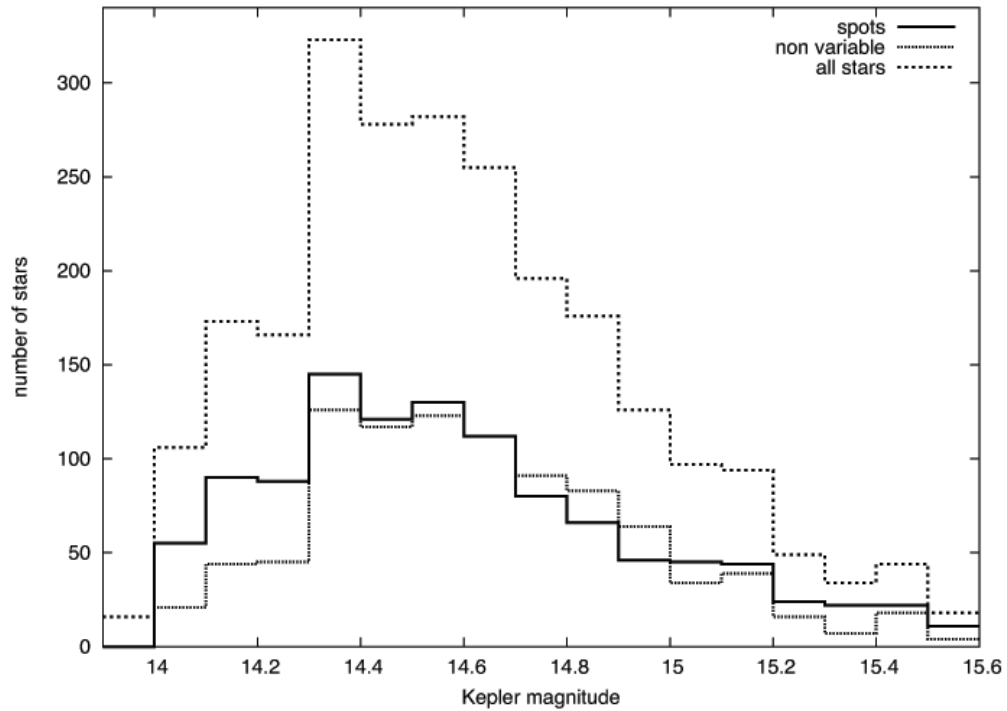


Fig. 2.— Histogram of our sample stars binned by *Kepler* magnitude (K_p). We include the entire sample (dashed line), the non-variable stars (dotted line), and rotating stars with spots (solid line). Stars are considered to be non-variable if there are no peaks visible in the FT greater than $30 \mu\text{mag}$. The number of stars reaches a peak near magnitude 14.4 and drops steadily towards fainter magnitudes.

corrected light curve files. These light curves have systematic error sources from the telescope and spacecraft removed (Thompson & Fraquelli 2012). We first analyzed the light curves of the stars with tested software written by J. Jackiewicz (McNamara et al. 2012). This software processes the light curves by removing bad data points (infinities and points more than three sigma away from neighboring points), converts from *Kepler* flux (electrons/sec) to parts per million (ppm) for each light curve using the formula $f(t) = 10^6((F_K/y) - 1)$ (where y is the mean of the entire light curve or a low-order polynomial fit to the light curve, depending on artifacts that are present in the light curve), performs a fast Fourier transform (FFT) on the light curve and plots the resulting power spectra on one page for ease of analysis. The results were visually inspected by at least two of the authors of this paper for variability. In addition, we analyzed the light curves with a locally created program that removed bad data points, converted from *Kepler* flux (electrons/sec) to parts per million (ppm) for each light curve, and performed a discrete FT (Deeming 1975). The results from the two methods were equivalent. We analyzed each quarter of data separately as well as all the quarters in one data set. This allowed us to be sure the variations were indeed from our target star and not from another star sharing the same pixels in one orientation of *Kepler* (which we found in a few cases). We did not perform any special stitching of data sets from one quarter to the next, since we are only interested in determining whether a star was variable and what type of variable star it is. We are less interested – for now – in the precise frequency or amplitude determinations, which would require care in how the light curves from each quarter are ”stitched” together.

Our analysis of the light curves and resultant FTs revealed that 1237 of the 2768 stars did not show significant light variability at the 30 μmag (or 30 ppm) amplitude level. The KIC numbers of these stars are listed in Table 1. The remaining 1531 stars show light curve variability of some sort. We discuss the variable stars further in the following subsections by type. We followed the criteria of Grigahc ene et al. (2010) and Uytterhoeven et al. (2011) in that we required stars to have at least three frequencies that are not obvious harmonics or combination peaks of each other (the exception is the HADS group; see below) to be classified as a γ Dor, δ Sct, or hybrid star candidate. We specifically excluded harmonic frequencies and frequencies below about 0.2 d^{-1} from consideration. The former peaks are not independent modes and periods over 5 days would almost certainly be due to rotation or binary motion. To do this, we visually examined the light curve, the FT, and examined the frequencies of the larger peaks in the FT. We have further criteria for accepting a star as a hybrid candidate, as discussed in the next section. We generally followed Balona et al. (2011) for the criteria for eclipsing binaries and rotating, spotted stars and these criteria are similar to that of Uytterhoeven et al. (2011). We also used the classification scheme of Balona et al. (2011) wherever possible to make the comparison of our results to theirs easier.

4. Discussion of Variable Stars

The Balona et al. (2011) study considered three types of γ Dor/ δ Sct variables. The first two types are γ Dor and δ Sct stars. In addition, some stars show both types of pulsation behavior simultaneously and are called hybrid stars. We classify a star as hybrid if it satisfies the following three criteria (see Grigahcène et al. (2010) and Uytterhoeven et al. (2011)): 1) frequencies are detected both in the δ Sct ($> 5\text{d}^{-1}$ or $> 58\mu\text{Hz}$) and gamma Doradus ($< 5\text{d}^{-1}$ or $< 58\mu\text{Hz}$) frequency regimes; 2) the amplitudes in the two regimes are roughly comparable (within a factor of 7); and 3) at least two frequencies (that are not obvious harmonics or combination frequencies) are found in each regime with amplitudes greater than 40 ppm. The T_{eff} and $\log g$ range for these stars also encompasses some other objects that show light curve variability. Contact eclipsing binary stars, especially W Ursae Majoris (W UMa) stars (contact binaries with both stars being typically early F spectral types) also fall into the hybrid star parameter space. We also found several detached eclipsing binaries and other types of binary star systems that will be discussed in more detail later.

Stars with rotationally modulated starspots can also lie in the same part of the T_{eff} and $\log g$ range as δ Sct, γ Dor, and hybrid stars. The spots can induce a near monotonic behavior or can show traveling wave patterns. The spots can also come and go in these stars, so the light curves can sometimes be irregularly modulated. Since most main-sequence stars in the δ Sct/ γ Dor region are fairly rapid rotators ($50 \text{ km s}^{-1} < v \sin i < 200 \text{ km s}^{-1}$), we expect the rotation periods to be between 0.5 and 2 days. Because the rotation frequency range overlaps the γ Dor pulsation frequency range, we require at least two frequencies (that are not obvious harmonics or combination frequencies) with sharp peaks before we can classify a star as being a γ Dor candidate. Our experience is that many rotating stars tend to show an indistinct cluster of low frequency peaks (the ROT category), although sometimes there are one (SPOTV) or two (SPOTM) fairly distinct peaks present; see the Rotationally Variable stars section for a description. When two peaks are present in a SPOTM star, one peak is the harmonic (twice the frequency) of the first due to the

Table 1. Nonvariable (amplitude < 30 ppm) stars found in our survey

KIC #	KIC #	KIC #	KIC #	KIC #	KIC #
1026536	1433534	2974588	2991687	3117547	3233511
3236044	3245621	3329462	3341092	3342912	3343104
3343915	3353469	3356332	3429786	3439956	3444020
3444187	3444426	3454000	3457689	3457925	3553769
3557803	3558758	3640389	3643325	3646321	3729981

Note. — Table 1 is published in its entirety in the electronic edition of the *Astronomical Journal*. A portion is shown here for guidance regarding its form and content.

non-sinusoidal pulse shape. The large number of possible mechanisms for light curve variability led us to create several categories of stars based on the morphology of the light curve, and we borrowed several of the categories from Balona (2011). In some cases, the light curve morphology is indicative of specific physical behavior, but in other cases the physical behavior cannot be uniquely determined. We list the types of stars and the number found in Table 2. We discuss representative members of each group below.

4.1. γ Dor Star Candidates

We detected 6 γ Dor candidate stars in our limited sample of 14 stars from Quarters 2 and 4, and another 201 candidate γ Dor stars in the larger sample, for a total of 207 stars. This is 13.4% of the variable stars. The γ Dor stars are identified in Table 3 by KIC number, *Kepler* magnitude K_p , T_{eff} , $\log g$, and category. The T_{eff} values have been adjusted upward by 200 K from the KIC catalog to account for the systematic temperature offset described by Pinsonneault et al. (2012). We have three categories, first described by Balona (2011). They are: ASYM, where the amplitude of the beat pattern above the mean level is considerably greater (about 2 times) than the amplitude below the mean level; the SYM category is similar to ASYM except that the excursions above and below the mean are nearly symmetric; and the MULT class shows a multitude of relatively low amplitude modes. We show three examples of our discoveries in Figure 3, with the light curve for a representative quarter in the left panel and the resultant FT in the right panel. KIC6128330 is a typical ASYM star whose maximum excursions about the mean are about three times the minimum excursions. KIC7191683 is a SYM star and the closely spaced frequencies in the FT result in a strong beat pattern in the light curve. Finally, KIC6210324 is a MULT star that has numerous FT peaks between 0.25 and 5 $c d^{-1}$. Our discoveries have frequency patterns ranging from simple patterns of a few modes to complicated FTs that indicate rich pulsators that will be promising for asteroseismology. Although the typical period range for γ Dor pulsations is 0.33 to 3 days, we saw some stars with multi-periodic pulsations longer than 3 days that looked identical to shorter period stars that we identify as γ Dor candidates. All of these stars were in our MULT category and none had periods longer than 4 days. While some of these candidates may indeed be γ Dor stars, some may also have rotating spots present, either along with pulsations or instead of pulsations. These stars deserve further scrutiny.

We plot our γ Dor (plus δ Sct and hybrid) stars on a T_{eff} , $\log g$ diagram in Figure 4. Most of our γ Dor stars lie on the cool side of the ground-based instability strip, although many lie within the strip as well. Some γ Dor stars are hotter than the γ Dor instability region, but all of these lie within the δ Sct instability region. This behavior was also seen by Balona et al. (2011, their Figure 4) and Uytterhoeven et al. (2011, their Figure 10b). We examined the amplitude distribution of our discoveries and find that the majority of them have peak mode amplitudes of 100 to 500 ppm, although significant numbers are found with amplitudes up to 10^4 ppm (0.01 mag).

Table 2. Morphological Classification of variable star types

Category	Sub-category	number
γ Dor (207 stars)	Asymmetric (ASYM)	33
	Symmetric (SYM)	88
	multiple periods (MULT)	86
δ Sct (84 stars)	High amplitude (HADS)	47
	multiple periods (MULT)	33
	"other"	4
Hybrid (32 stars)	γ Dor dominant	7
	δ Sct dominant	7
	roughly equal	18
Binary (76 stars)	EA (detached)	17
	EB (contact)	52
	"transit"	4
	"heartbeat"	3
Rotation (1132 stars)	SPOTV (dominant period)	75
	SPOTM (traveling wave)	109
	ROT (dominant low frequency)	844
	VAR (low amplitude, type unknown)	103

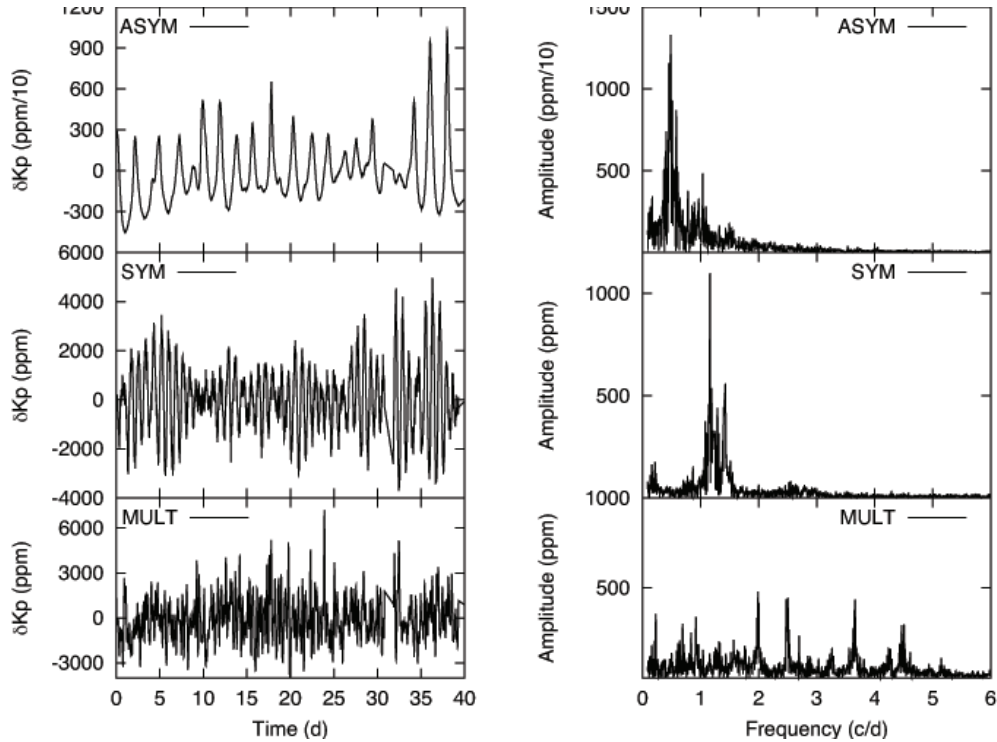


Fig. 3.— Light curves (left panels) and Fourier Transforms (right panels) for three representative γ Dor star candidates. KIC6128330 (top row) is an example of an ASYM star, KIC7191683 (middle row) is a SYM star, and KIC6210324 is an example of a MULT star. Note the different FT of the MULT star compared to the ASYM and SYM stars.

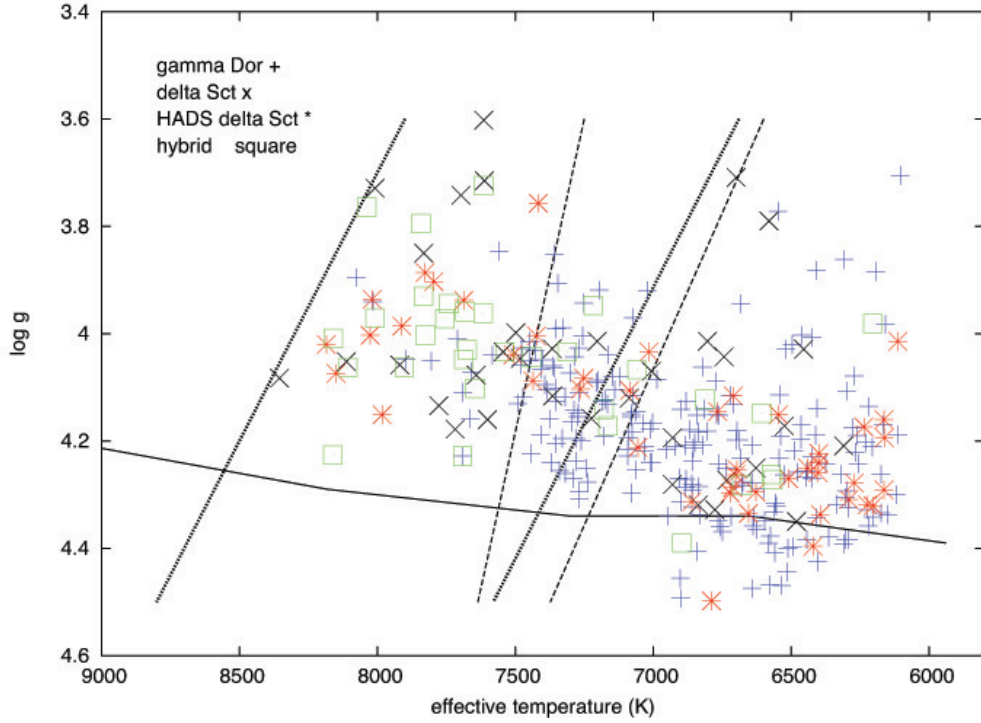


Fig. 4.— Location of the γ Dor, δ Sct, and hybrid star candidates from our sample in the T_{eff} , $\log g$ diagram. The ground-based δ Sct (thick dotted lines) and γ Dor (thin dashed lines) instability strips are indicated, along with the zero-age main sequence (solid line). The γ Dor star candidates are blue “+” signs, δ Sct star candidates are black “x” signs, high-amplitude δ Sct (HADS) star candidates are red “*” signs, and hybrid star candidates are green squares. There are no variable stars hotter than the δ Sct blue edge, and there are relatively few γ Dor star candidates hotter than the γ Dor blue edge.

4.2. δ Sct Star Candidates

In our study, we find 81 candidate δ Sct stars (and 3 more candidates in our limited sample of 14 stars, for a total of 84 candidate stars, or 5.4% of the variable stars). The δ Sct candidate stars are identified in Table 4 by KIC number, *Kepler* magnitude K_p , T_{eff} , $\log g$, and category. We use three classifications of δ Sct stars here. HADS stands for High Amplitude δ Sct Stars. Many of these are monoprotic, but the short (< 6 hour) period of the dominant peak implies that the dominant peak cannot be binary orbital period or rotation period due to the impossibly high velocities (but see the discussion below). The next class is MULT, which covers the objects with a rich spectrum of pulsation modes. Stars that do not fall in either of these two categories are called “other”. We show three examples of our discoveries in Figure 5, with the light curve for a representative quarter in the left panel and the resultant FT in the right panel. KIC2581626 is a multiperiodic HADS whose closely spaced modes leads to strong beating in the light curve. Second, KIC 5707205 is a MULT star that has several bands between 8 and 18 $c d^{-1}$. Finally, KIC 6304420 is in the “other” category. There are two dominant frequency bands that result in a strongly modulated light curve. Our discoveries have frequency patterns ranging from simple patterns of a few modes to complicated FTs that indicate rich pulsators that will be promising for asteroseismology.

We plot our δ Sct star candidates on a T_{eff} , $\log g$ diagram in Figure 4. Most of our δ Sct star candidates lie on the cool side of the ground-based δ Sct instability strip, although many lie within the strip as well. We found far more cool δ Sct star candidates than was seen by Balona and Dziembowski (2011, their Figure 1) and Uytterhoeven et al. (2011, their Figure 10b). Our HADS stars have many (40 of 47) stars that show a single dominant peak (typically between 4 and 6 $c d^{-1}$), along with a small peak at half the frequency of the dominant peak and at least one harmonic peak. If the small peak (at half the frequency of the dominant peak) is the rotation frequency of a spotted star, then the implied rotation velocities are 150 to 250 km s^{-1} , which is physically plausible. We note that Balona (2011) also found that the dominant low frequency mode appears to be twice the rotation frequency. The remaining δ Sct star candidates would have a temperature distribution peaked between 6500 and 8000 K, which would be closer to that of Balona and Dziembowski (2011) and Uytterhoeven et al. (2011). Spectroscopic observations of rotationally broadened absorption lines in our HADS candidates will be required to confirm this hypothesis.

We also examined the amplitude distribution of our discoveries and find a bimodal distribution. The multiperiodic stars comprise the entire sample with amplitudes below 10^4 ppm (0.01 mag) and only one star has an amplitude greater than this. By our definition, the HADS stars have amplitudes greater than 10^4 ppm (0.01 mag) and there are 42 of these (half of our discoveries), while 9 stars have amplitudes greater than 10^5 ppm (0.1 mag). If we compare our amplitude distribution to Balona and Dziembowski (2011), we find a dearth of pulsators with amplitudes below 1000 ppm. It is possible that short cadence data might find additional low amplitude and/or short period δ Sct stars. We note, however, that our sample (see Figure 1) contains relatively few stars between 7000 and 8000 K below magnitude 14 (for our contamination factor of < 0.05), suggesting that there

just are not any more hot stars available, probably because these stars are far enough away that they lie between spiral arms in our Galaxy (see discussion in Section 4.6).

Table 3. γ Dor star candidates found in our survey

KIC #	K_p	T_{eff}	$\log g$	class	Freq. Range	Ampl. high	Freq. high
					(d^{-1})	(ppm)	(d^{-1})
2167444	14.1	7140	4.1	MULT	0.5 – 5.2	1730	0.8082
2448307	14.0	7350	3.9	MULT	0.2 – 3.5	1390	1.2516
2579595	14.1	7150	4.1	ASYM	0.7 – 1.7	5175	1.2205
2581964	14.0	7410	4.2	ASYM	0.4 – 1.5	5914	0.5389
2857178	14.6	7440	4.2	ASYM	0.9 – 2.0	392	1.7313
2974858	14.4	7010	4.2	MULT	0.75 – 3.1	49	2.0287

Note. — Table 3 is published in its entirety in the electronic edition of the *Astronomical Journal*. A portion is shown here for guidance regarding its form and content. “Ampl. high” and “Freq. high” refer to the amplitude and frequency of the highest amplitude mode in the FT. The T_{eff} and $\log g$ values are rounded from the *Kepler* input catalog.

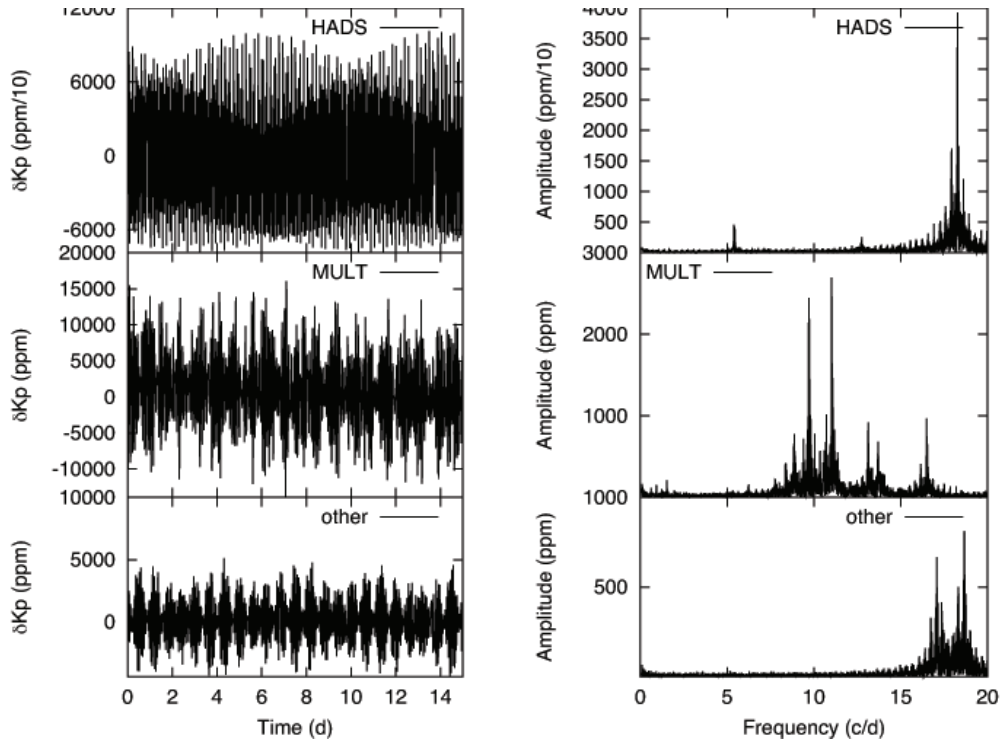


Fig. 5.— Light curves (left panels) and Fourier Transforms (right panels) for three representative δ Sct star candidates. KIC2581626 (top row) is an example of a HADS star, KIC5707205 (middle row) is an example of a MULT star, and KIC6304420 (bottom row) is an “other” star.

Table 4. δ Sct star candidates found in our survey

KIC #	K_p	T_{eff}	$\log g$	class	Freq. Range (d^{-1})	Ampl. high (ppm)	Freq. high (d^{-1})
2581626	15.0	8030	4.0	HADS	18.2 – 18.3	18,090	18.2553
2972514	14.0	6550	4.2	HADS	3.95 – 4.05	57,465	3.9993
3119295	14.3	7440	4.1	HADS	4.55 – 4.65	49,230	4.5944
3953144	14.7	8150	4.1	HADS	8.0 – 18.5	8680	9.9374
4036687	15.2	6400	4.2	HADS	6.7 – 6.8	28,080	6.7302
4066203	14.1	6700	4.3	HADS	5.65 – 5.75	14,250	5.7163
4243668	14.7	6510	4.3	HADS	5.2 – 5.3	10,060	5.2646
4374279	14.6	7060	4.2	HADS	5.85 – 5.95	4000	5.9070
4466691	14.3	6710	4.3	HADS	4.1 – 4.2	28,980	4.1723
4547067	14.7	6240	4.2	HADS	4.9 – 5.0	14,190	4.9662
4651526	14.8	6440	4.2	HADS	6.7 – 6.8	22,055	6.7715
4995588	15.0	7600	4.2	other	23.5 – 24.0	4300	23.7488
5027750	14.8	6930	4.2	MULT	10.0 – 24.0	2670	11.8209
5284701	14.4	7720	4.2	MULT	15.2 – 24.0	760	19.3581
5286485	14.8	6840	4.3	MULT	7.6 – 10.1	4270	10.0890
5353653	15.1	6710	4.1	HADS	5.45 – 5.55	11,205	5.4730
5357882	14.7	6630	4.3	HADS	5.15 – 5.25	21,745	5.2004
5534340	14.6	7250	4.1	HADS	5.4 – 16.0	12,280	6.0612
5611763	14.9	6400	4.2	HADS	5.55 – 5.65	15,260	5.5868
5707205	14.3	7220	4.2	MULT	6.0 – 17.0	7890	9.7293
5788165	14.4	8110	4.1	MULT	8.0 – 23.0	3670	17.9811
5966237	14.9	6790	4.5	HADS	5.05 – 5.15	11,780	5.0919
5978805	14.1	6740	4.0	other	21.2 – 24.0	250	23.7209
6271512	14.2	7830	3.9	HADS	10.3 – 10.4	8300	10.3721
6304420	14.4	7480	4.0	MULT	16.9 – 18.6	1500	18.5395
6344429	14.7	7020	4.0	HADS	4.85 – 4.95	12,600	4.8972
6442207	15.5	7980	4.2	HADS	4.35 – 4.45	11,000	4.4000
6444630	14.6	6160	4.2	HADS	6.0 – 6.1	4200	6.0558
6672071	14.9	6200	4.3	HADS	5.65 – 5.75	100,000	5.7070
6696050	14.3	7830	3.8	MULT	12.0 – 12.1	2000	12.028
6778487	14.8	6420	4.4	HADS	5.05 – 5.15	91,000	5.095
6836820	14.5	6270	4.3	HADS	4.4 – 4.5	110,000	4.4720
6870432	14.0	7090	4.1	MULT	20.7 – 20.8	1500	20.772
6955650	14.2	7510	4.0	HADS	3.75 – 3.85	4100	3.7967
7048016	14.0	6480	4.4	MULT	16.0 – 16.1	5470	16.0597
7124161	14.7	7690	3.9	HADS	4.65 – 4.75	25,000	4.6869
7347529	14.1	7610	3.6	MULT	11.2 – 11.8	654,900	11.7416
7381616	14.5	6930	4.3	MULT	8.8 – 22.0	3800	15.014
7521682	14.8	6660	4.3	HADS	5.55 – 5.65	7120	5.609
7601767	14.5	6770	4.1	HADS	4.05 – 4.15	88,600	4.1121
7617649	14.6	6160	4.3	HADS	5.4 – 5.5	175,000	5.433
7668283	14.6	7420	3.8	HADS	3.65 – 3.75	12,500	3.7143
7750215	14.3	8360	4.1	MULT	15.2 – 23.0	5795	16.4151
7905603	14.3	7500	4.0	MULT	7.9 – 18.5	9235	18.233
7937097	14.3	6220	4.3	HADS	4.65 – 4.75	7300	4.6869

Table 4—Continued

KIC #	K_p	T_{eff}	log g	class	Freq. Range	Ampl. high	Freq. high
7948091	14.8	6290	4.3	HADS	6.5 – 6.6	3330	6.526
7984934	14.1	6160	4.2	HADS	6.8 – 6.9	19,500	6.874
8052082	14.6	6780	4.3	MULT	15.9 – 24.0	1145	18.3534
8087649	14.4	7260	4.1	HADS	4.1 – 4.2	4700	4.1682
8090059	14.0	8020	3.9	HADS	18.3 – 18.4	4750	18.3534
8144212	14.2	7360	4.1	MULT	9.3 – 9.4	1600	9.349
8150307	14.8	7440	4.1	HADS	14.65 – 14.75	4500	14.6977
8245366	11.2	N.A.	N.A.	MULT	6.9 – 12.2	808,370	11.9743
8248296	14.1	7920	4.1	MULT	10.4 – 22.8	465	13.556
8248967	15.1	6720	4.3	HADS	3.3 – 3.4	15,000	3.3715
8249829	14.3	7090	4.1	HADS	16.7 – 16.8	2450	16.7814
8315263	14.3	7700	3.7	MULT	13.0 – 18.8	7300	13.2372
8322016	14.1	6800	4.0	other	14.4 – 24.5	200	24.0372
8323981	14.3	8010	3.7	MULT	8.0 – 23.2	120	20.4372
8393922	14.0	7540	4.0	MULT	9.8 – 22.0	2000	13.0791
8508096	14.2	7420	4.0	HADS	22.1 – 22.2	1500	22.1209
8516900	14.2	6580	3.8	MULT	5.0 – 20.0	2600	16.3628
8648251	14.6	6520	4.2	MULT	15.1 – 19.6	5240	15.1256
8649814	14.4	6700	3.7	MULT	7.6 – 15.6	5685	7.600
8960514	14.4	6730	4.3	MULT	6.65 – 6.75	3100	6.6977
8963394	14.5	6110	4.0	HADS	5.3 – 5.4	11,840	5.3581
9075949	14.6	6400	4.3	HADS	5.65 – 5.75	10,930	5.6837
9077483	15.4	6400	4.3	HADS	5.4 – 5.5	25,155	5.4276
9137819	15.0	7800	3.9	HADS	3.6 – 3.7	17,410	3.6595
9202969	14.0	6700	4.3	HADS	4.95 – 5.05	4310	4.9810
9214444	14.2	7610	3.7	MULT	8.1 – 24.0	540	21.6372
9364179	14.1	7200	4.0	MULT	18.0 – 20.0	1235	18.200
9594857	11.0	N.A.	N.A.	MULT	5.0 – 10.0	862,070	9.9695
9613175	14.2	7370	4.0	MULT	18.7 – 24.0	330	20.6741
9613575	14.4	6310	4.2	MULT	8.5 – 24.0	3360	13.1628
9614153	14.2	6460	4.0	MULT	10.0 – 16.4	2270	13.2186
9700322	12.7	N.A.	N.A.	HADS	9.6 – 12.6	392,840	12.6259
9706609	14.1	7640	4.1	MULT+rot	5.0 – 9.0	420	7.3767
9724292	14.4	7010	4.1	MULT	10.8 – 16.4	2810	13.8000
9942562	14.6	6630	4.2	other	6.75 – 6.85	550	6.8000
10451090	9.2	7780	4.1	MULT	10.0 – 20.0	31,050	10.6695
11143576	15.1	8180	4.0	HADS	15.7 – 15.8	6480	15.7719
11704101	15.4	6860	4.3	HADS	5.8 – 5.9	959,070	5.8527
11852985	14.4	7910	4.0	HADS	19.85 – 19.95	10,455	19.8915

Note. — “Ampl. high” and “Freq. high” refer to the amplitude and frequency of the highest amplitude mode in the FT. The T_{eff} and log g values are rounded from the *Kepler* input catalog.

4.3. Hybrid Star Candidates

We discovered one hybrid star candidate in our limited sample of 14 objects and only 31 hybrid candidates in our larger sample. Thus, the hybrid stars constitute 2.1% of the variable star candidates. We use three classifications: γ Dor-dominated FTs, δ Sct-dominated FTs, and ones where the γ Dor and δ Sct amplitudes are within a factor of three of each other and are placed in the “equal” bin. The hybrid star candidates are identified in Table 5 by KIC number, *Kepler* magnitude K_p , T_{eff} , $\log g$, and category. We show three of the hybrid stars from our limited data sample in Figure 6, in two columns. KIC5561007 is representative of our γ Dor-dominated hybrid star candidates, while KIC3657237 is one of the few δ Sct-dominated hybrid star candidates. KIC2855026 has prominent peaks from 1 to 20 c d^{-1} and is in the “equal” amplitude category. We plot our hybrid star candidate discoveries on a T_{eff} , $\log g$ diagram in Figure 4. Most of our hybrid star candidates lie within the ground-based δ Sct instability strip, although one-third lie on the cool side of the instability strip. This is in marked contrast to the γ Dor and δ Sct stars. This behavior was also seen by Uytterhoeven et al. (2011, Figure 10b). In addition, the amplitude distribution of our hybrid stars shows that almost all have peak mode amplitudes below 3000 ppm in both the δ Sct and γ Dor range. The relatively low mode amplitude works against our being able to detect faint (fainter than magnitude 15) hybrid stars.

We note that Bouabid et al. (2013) showed that some stars whose frequency distribution would lead to a hybrid classification could in fact be rapidly rotating γ Dor stars whose g-modes have been shifted to higher frequencies. Multi-color photometry and/or spectroscopic observations would be needed to determine the p - or g -mode nature of the modes and confirm whether a hybrid star candidate of ours is truly a hybrid star.

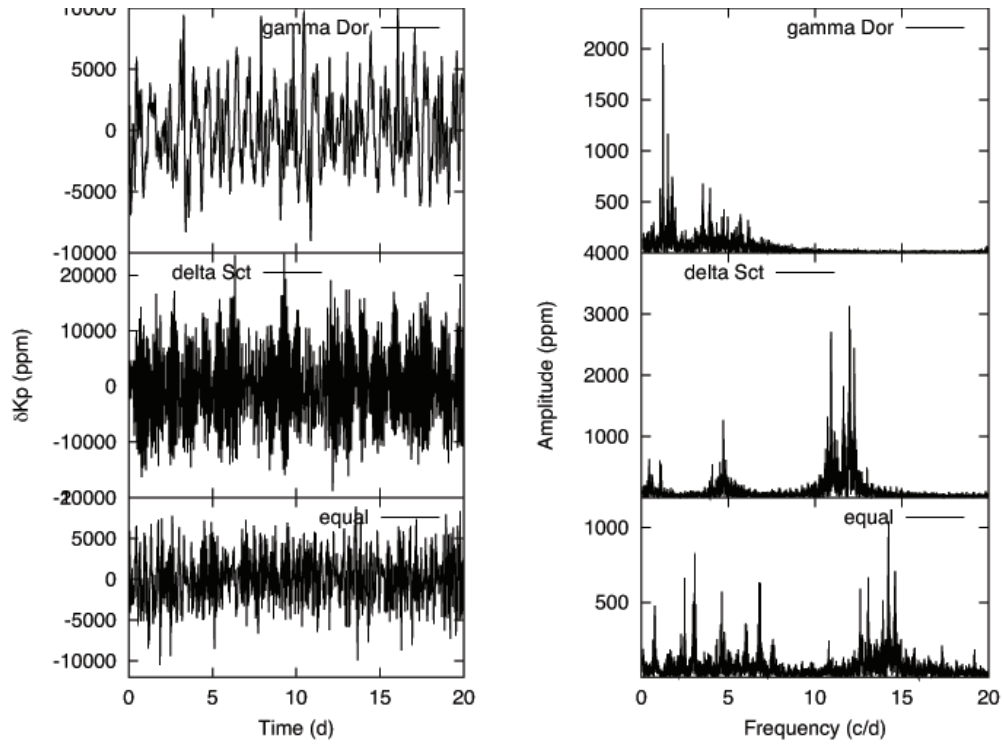


Fig. 6.— Light curves (left panels) and Fourier Transforms (right panels) for three representative hybrid star candidates. KIC5561007 (top row) is a γ Dor dominant star, KIC3657237 (middle row) is a δ Sct dominant star, and KIC2855026 (bottom row) is an example of a star with near equal amplitudes in the γ Dor and δ Sct ranges.

Table 5. Hybrid star candidates found in our survey

KIC #	K_p	T_{eff}	log g	class	γ Dor Ampl.	γ Dor Freq.	δ Sct Ampl.	δ Sct Freq.
					(ppm)	(d^{-1})	(ppm)	(d^{-1})
2301163	14.3	7540	4.0	γ Dor	8175	2.1076	8925	19.7405
2855026	14.1	7690	4.0	equal	855	3.0374	1665	17.3012
3456100	14.1	8040	3.8	δ Sct	168	1.5304	1320	17.2411
3657237	14.3	6570	4.3	δ Sct	600	1.0312	4585	11.9070
3941524	14.1	7680	4.0	equal	45	1.0537	180	23.6279
4668676	14.1	6900	4.4	δ Sct	1900	1.9743	6865	15.3581
4999763	15.0	7760	4.0	equal	1295	1.3190	560	19.7767
4999789	15.0	7650	4.1	equal	940	1.6495	2720	15.4884
5018191	14.5	7160	4.2	δ Sct	225	0.5238	2055	10.4465
5466537	10.3	7180	4.1	δ Sct	205	2.7857	1080	22.2605
5553489	14.4	6680	4.3	γ Dor	150	1.0631	45	5.1238
5561007	14.2	7690	4.2	γ Dor	2075	0.9766	645	5.6465
5771101	15.0	7440	4.0	equal	720	0.7126	1135	7.8512
5809732	14.1	6810	4.1	equal	125	1.7827	80	8.4279
5966212	15.1	7680	4.0	equal	305	1.9121	800	15.8326
6130261	14.9	7830	3.9	γ Dor	3455	0.9930	590	21.7674
6290877	14.1	8010	4.0	equal	395	2.1051	885	16.7163
6460258	14.2	7060	4.1	γ Dor	2770	2.9810	365	5.1429
6467349	14.6	6610	4.1	equal	690	1.6005	1200	18.7814
6586020	15.1	7310	4.0	equal	425	3.2103	810	17.5814
6936178	14.4	8160	4.0	equal	45	1.8972	100	17.6930
6960727	14.1	8160	4.2	δ Sct	125	2.1168	600	18.8000
6974847	14.5	7840	3.8	δ Sct	500	1.4159	1825	17.9256
7300263	14.5	6200	4.0	equal	75	2.0958	140	17.8419
7302192	14.5	6570	4.3	equal	275	1.5818	725	15.8233
7354531	14.5	7620	3.7	equal	1440	1.2406	1890	13.0419
7750216	14.0	8110	4.1	δ Sct	340	0.6519	750	22.2140
8314246	14.0	7220	3.9	equal	2350	1.8037	2600	14.1302
9005210	14.0	7740	3.9	equal	625	1.4650	1200	14.5953
9402020	15.1	7620	4.0	γ Dor	290	2.1449	170	19.4977
9529640	14.5	7830	4.0	equal	355	2.3575	700	21.6000
10134571	14.6	7900	4.1	equal	80	2.4418	190	21.6279

Note. — “ γ Dor Ampl.” and “ γ Dor Freq.” refer to the amplitude and frequency of the highest amplitude mode in the γ Dor region ($< 5 \text{ d}^{-1}$) of the FT, while “ δ Sct Ampl.” and “ δ Sct Freq.” refer to the amplitude and frequency of the highest amplitude mode in the δ Sct region ($> 5 \text{ d}^{-1}$) of the FT. The T_{eff} and log g values are rounded from the *Kepler* input catalog.

4.4. Binary Stars

We find 73 binary stars in our sample (and 3 more in our 14 star sample from Q2 and Q4), which is 4.9% of our variable star sample. The binary stars are identified in Table 6 by KIC number, *Kepler* magnitude K_p , T_{eff} , $\log g$, category, and orbital period (in days). Some of the stars show clear eclipses, although many show ellipsoidal variations that indicate two distorted stars seen from different positions as they orbit each other, to partially eclipsing distorted stars. We classified these stars into four categories (Balona 2011), with unphased light curve examples shown in Figure 7. The “EA” stars are detached binaries that show obvious eclipses, but no ellipsoidal effects, as shown by KIC8690001 in panel 1, which also obviously has an eccentric orbit. The orbital periods range from 1.3 to 24.1 days. The “EB” stars are contact (or ellipsoidal) eclipsing binaries, such as KIC2161023 in panel 2. Many of them have periods of less than 1 day, making them likely W UMa stars. The longest period for any of these is 3.72 days, so they are clearly very tight binaries (semimajor axis $< 10^7$ km). These are binary stars in eccentric orbits where the stars become tidally distorted near periastron passage, causing a sudden rise in the light curve. The three stars have periods of 9.5, 12, and 23 days. KIC6963717 is the heartbeat star illustrated in the third panel. There are four stars labeled “transit” that have irregular light curves (due to starspots or rotation) punctuated by narrow eclipses, as shown by KIC7599004 in the bottom panel. The periods between the minima range from 4.9 hr to 5.5 d. We are not claiming that they are transits by dark objects, but we believe they are binary objects of some sort. We compared our list of binary stars to the *Kepler* binary star database (current as of 3/31/2014) and found that 44 of our stars are not in this list. We highlight the new discoveries in boldface text in Table 6. To the extent that the KIC photometric T_{eff} and $\log g$ values have meaning for binary stars, they are uniformly distributed in T_{eff} , while the $\log g$ value increases with decreasing T_{eff} . We refer the reader to Gaulme and Guzik (2014), who performed a more detailed analysis of these stars.

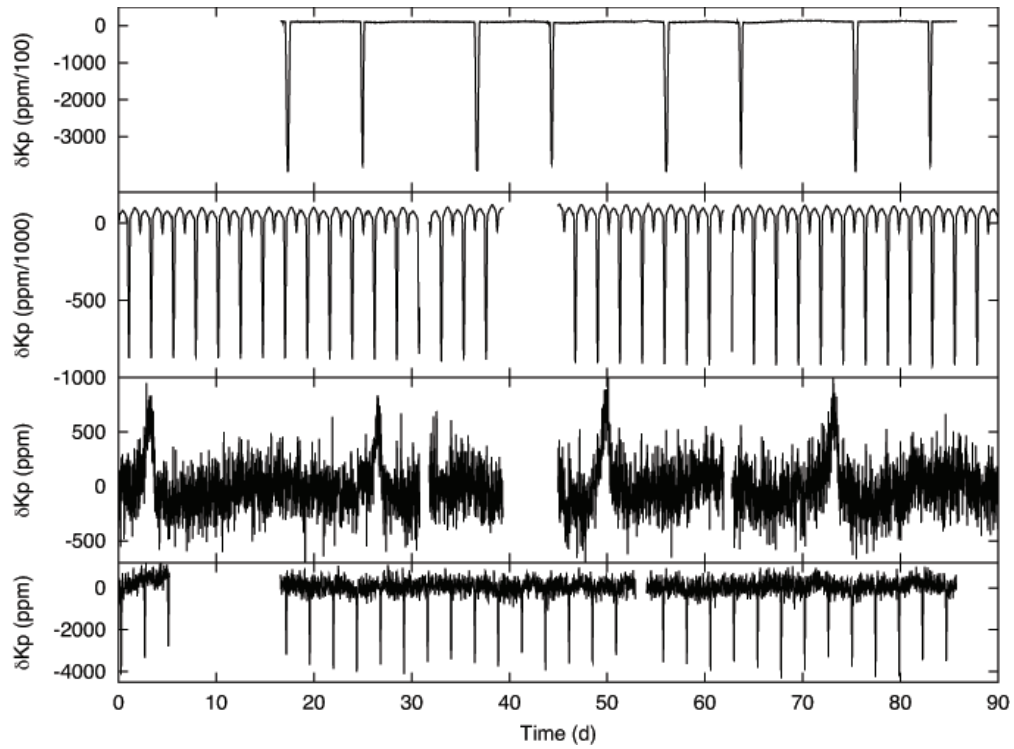


Fig. 7.— Unphased light curves for four representative binary stars. KIC8690001 (top row) is an example of an EA (detached binary) star, KIC2161623 (second row) is an EB (ellipsoidal eclipsing binary) star, KIC6963171 is a “heartbeat” star with tidal distortion near periastron passage causing the sharp rises at 3, 27, 50, and 73 days, and KIC7599004 is an example of a “transit” star with low amplitude eclipses.

Table 6. Binary stars found in our survey

KIC #	K_p	T_{eff}	$\log g$	class	Per (d)
1433410	14.1	6200	4.0	EB	0.283
2161623	14.3	6710	4.1	EB	2.283
2449084	15.0	6380	4.4	EB	0.740
2719436	14.0	7240	4.1	EB	0.740
2988984	15.3	7360	4.1	EB	0.713
3547111	14.4	6600	4.3	EB	1.208
3633901	14.9	7380	4.2	EB	0.807
4160006	14.3	6120	4.2	EA	2.037
4470124	14.9	6460	4.4	heartbeat	11.433
4554004	15.1	6410	4.2	EB	0.743
4570326	9.8	N.A.	N.A.	EB	1.122
4739791	14.7	7740	3.9	EA+pulse	0.899
4815612	15.2	6590	4.3	EA	3.857
4936680	14.3	8100	4.0	EB	0.666
5022908	14.3	6900	4.1	EB	0.637
5036966	14.3	6160	4.1	EB	62.735
5290305	14.3	6740	4.3	EB	0.621
5357682	14.6	6640	4.2	EB	0.718
5358200	15.0	7230	4.0	EB	0.536
5461570	14.8	7330	4.0	EB	0.508
5524325	15.0	7380	4.0	EB	0.626
5606644	14.8	7740	4.2	EA	0.862
5615815	14.8	7330	4.1	EB+pulse	0.674
5616194	15.0	6580	4.2	EA	0.623
5858519	14.7	6130	4.3	EA	4.182
5878081	14.4	7900	3.8	EB+pulse	0.591
5962514	14.8	6770	4.3	EB	1.585
6048106	14.1	6980	4.2	EB	1.556
6220497	14.7	7450	3.9	EB	1.332
6224853	14.4	7540	4.1	EB	0.535
6948815	15.3	7630	4.0	EB	1.556
6963171	14.1	6130	3.9	heartbeat	23.3
7025851	14.4	6250	4.3	EA	4.681
7107567	14.2	7100	4.2	transit	0.809
7108433	15.1	7410	4.1	EB	1.527
7365447	14.3	6800	4.3	EA	2.471
7377343	14.4	6160	4.3	EA	8.40
7436177	14.6	6270	4.3	EA	10.50
7599004	14.8	6320	4.2	transit	2.40
7700578	14.2	6890	4.1	EB	1.505
7740302	12.0	N.A.	N.A.	EB	1.154
8153568	15.1	7000	4.1	EA	3.652
8182360	15.3	7100	4.1	EB	0.697
8183540	14.3	6630	4.2	EB	0.343
8240861	15.3	6290	4.2	EB	0.901
8294484	14.7	6450	4.3	EB+spot	1.013

Table 6—Continued

KIC #	K_p	T_{eff}	log g	class	Per (d)
8380743	14.0	6170	4.0	EB	2.024
8455359	14.2	6840	4.0	EB	2.959
8565912	14.7	6970	4.1	EB	1.012
8579812	14.8	6720	4.1	EB	0.658
8587078	14.0	6240	4.0	EB	0.583
8690001	14.3	6140	3.9	EA	19.2
8696327	14.6	6920	4.1	EB	0.875
8736072	14.9	8030	4.1	EB	0.477
8822555	14.4	6580	4.3	EB	0.852
8895509	14.2	6260	3.8	heartbeat	9.767
8904714	14.8	6120	4.1	transit	5.25
9101400	14.7	6610	4.3	EB	1.647
9108058	14.3	6760	4.1	EB	2.176
9205993	14.9	7320	4.1	EB	1.226
9282687	14.1	6820	4.1	EB	1.680
9291368	14.0	8090	3.7	EB	3.717
9343862	15.0	7910	4.0	EB	1.120
9479460	14.7	7770	3.7	EB	2.089
9514070	15.2	6790	4.1	EB	0.607
9658118	14.2	6420	4.3	EA	24.06
9767392	14.7	6600	4.2	EA	1.462
9832545	15.2	8100	3.9	EB	1.012
9843435	14.8	7490	4.1	EB	1.680
9899345	15.0	6800	4.1	transit	1.333
9936698	14.0	6590	4.2	EA	5.712
9954225	14.6	6290	4.2	EB	1.324
10141087	15.2	6620	4.2	EB	0.469
11401845	14.4	7790	3.9	EA	2.161
11819135	15.1	6900	4.1	EB+pulse	1.902
11867071	14.3	6600	4.4	EA+pulse?	2.964

Note. — KIC numbers in **boldface** are binary systems discovered in this study. The T_{eff} and log g values are rounded from the *Kepler* input catalog.

4.5. Rotating Stars

This class has stars that show starspots moving with rotation, and other sources of long-term frequency modulation. The rotating stars are identified in Table 7 by KIC number, *Kepler* magnitude K_p , T_{eff} , $\log g$, and category. It is the single biggest class of variable stars in our sample, with 1132 members, or 74.0% of the variable stars we found. The large number of rotationally modulated stars is a reflection of the cooler stars in our sample. We show three representative examples in Figure 8. The SPOTM category (represented by KIC3545661) shows a clear beat pattern (the light curve in Figure 8 is not long enough to fully show the beat cycle) and two dominant peaks in the FT. The modulated light curves are likely due to multiple spots rotating in and out of view. The SPOTV category (represented by KIC4276984) has a single dominant peak in the FT and shows a repeating light curve that can be explained by a single spot rotating in and out of view. The ROT category shows low frequency (typically $< 1 \text{ c d}^{-1}$) power in the FT and a modulated light curve (KIC3248536 is an example), but no clear peaks in the FT like the SPOTM and SPOTV stars. Their variations may be due to rotation, but if so, the spots are not stable for more than a few rotation periods. Finally there are a number of stars that show low frequency variability, but with no clear period in the light curve or the FT. We labeled such stars as VAR, but we cannot ascribe an obvious physical mechanism to the variations. We show the distribution of our rotating stars in a T_{eff} , $\log g$ diagram in Figure 9. As seen in Figure 9, almost all of these objects are cooler than the red edge of the γ Dor instability strip. The cool effective temperatures are consistent with rotation, since this implies the presence of deep convection zones that would produce strong magnetic activity cycles. We note that a few stars are within (or are even hotter) than the δ Sct instability strip. Balona (2013) discusses instances of such stars in his sample. Our sample of nine stars with clearly identifiable peaks has properties similar to those of Balona (2013) in that two of the nine (22%) have the harmonic peak as the highest amplitude (Balona 2013 has 25%). Eight of our nine stars have implied rotational velocities (based on the fundamental mode frequency and KIC radius values) between 20 and 265 km/s. One star has a rotation velocity of 1.8 km/s; this could be a horizontal branch star. Given our small number of stars, the distribution is similar to Figure 8 in Balona (2013). Thus, our nine stars are also likely to be A-type stars with some sort of rotating feature, such as starspots.

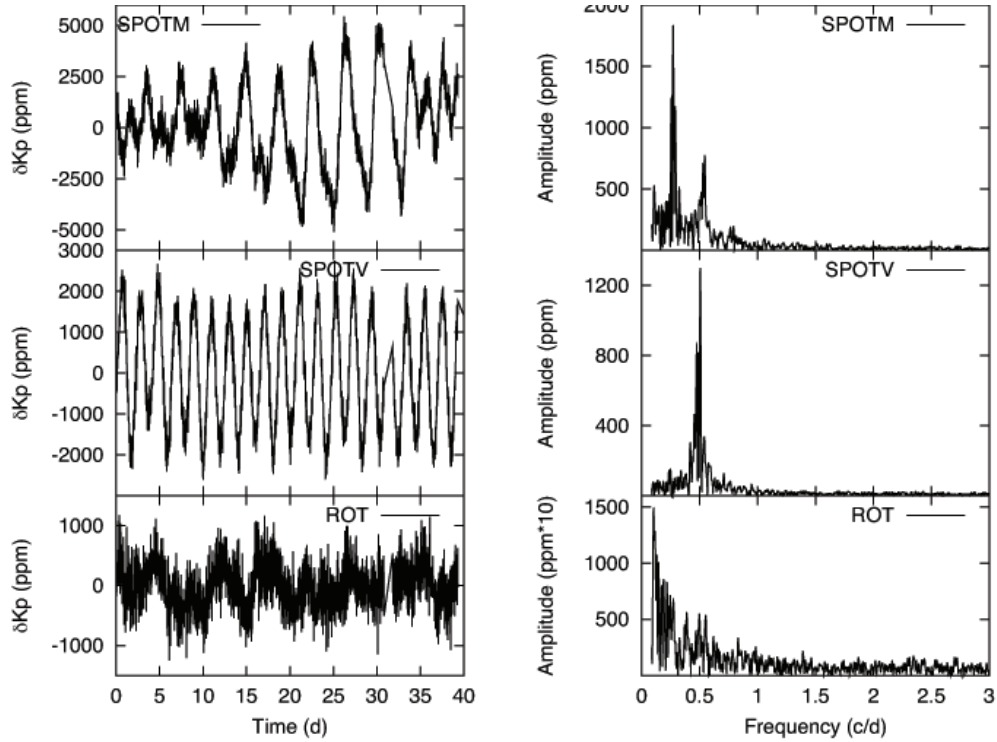


Fig. 8.— Light curves (left panels) and Fourier Transforms (right panels) for three representative rotating, spotted stars. KIC3545661 (top row) is an example of a SPOTM star with multiple spots and frequencies, KIC4276984 (middle row) is a SPOTV star with a single dominant period, and KIC3248536 is a ROT star with multiple frequencies below $1 c d^{-1}$.

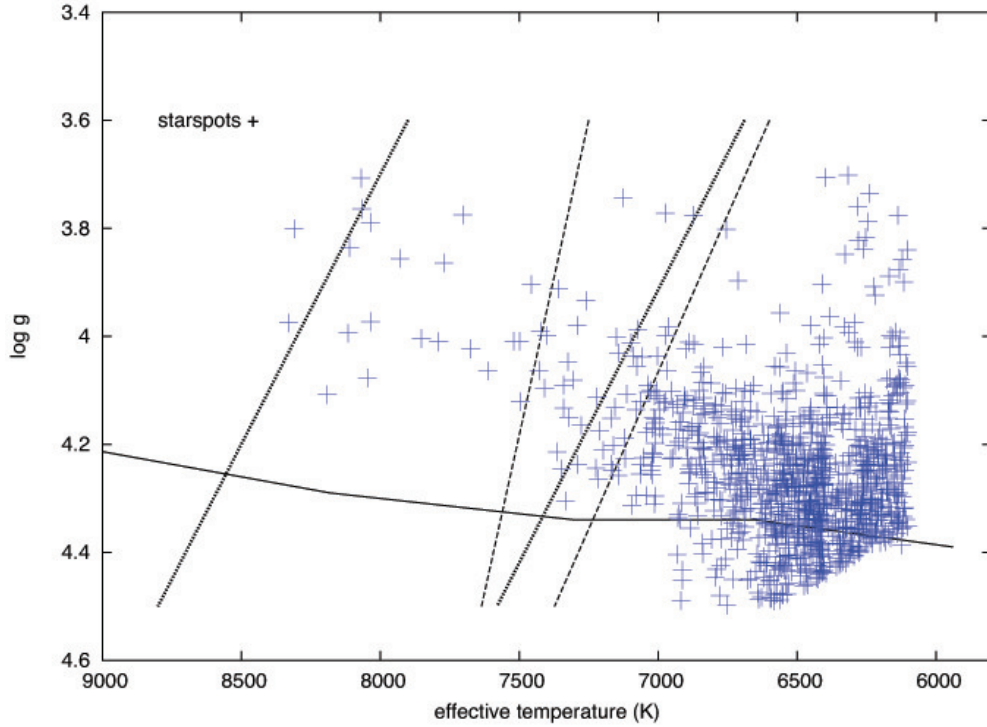


Fig. 9.— Location of the rotating, spotted stars from our sample in the T_{eff} , $\log g$ diagram. The ground based delta Scuti (thick dotted lines) and γ Dor (thin dashed lines) instability strips are indicated, along with the zero-age main sequence (solid line). These stars are almost all cooler than the instability strips, as one would expect, since stellar activity (spots) become more prevalent with cooler T_{eff} values (and deeper envelope convection zones). The cutoffs at 6200 K and in $\log g$ are observational selection effects of our sample.

Table 7. Rotating stars found in our survey

KIC #	K_p	T_{eff}	log g	class
1160919	14.2	6160	4.0	SPOTV
1296334	14.9	6670	4.1	ROT
1572948	14.5	6560	4.1	VAR
1720794	14.5	6280	4.1	ROT
2975747	14.0	6430	4.4	VAR
2985386	14.0	6450	4.2	ROT

Note. — Table 7 is published in its entirety in the electronic edition of the *Astronomical Journal*. A portion is shown here for guidance regarding its form and content. The T_{eff} and log g values are rounded from the *Kepler* input catalog.

4.6. Comparison of γ Dor, δ Sct, and hybrid candidate star discovery rates

In this section we discuss the discovery rate of our pulsating stars, comprised of γ Dor, δ Sct, and hybrid star candidates. Our γ Dor candidate discovery rate ($\equiv \gamma$ Dor stars/pulsating stars) is about 64%, the δ Sct candidate star discovery rate is 26%, and hybrid star candidates comprise the remaining 10%. The magnitude distribution of our γ Dor stars has a peak at magnitude 14.3 and only 18 stars are fainter than magnitude 15 (see Figure 10). This magnitude distribution is similar to the magnitude distribution of the entire sample, however. The magnitude distribution of our δ Sct candidate stars is essentially flat between magnitude 14.0 and 14.8 (see Figure 10), while only 7 are magnitude 15 or fainter (all of these are HADS stars). There is also a dearth of faint hybrid stars in our sample. We find that 22 of the 32 hybrid stars lie between magnitudes 14.0 and 14.5 (see Figure 10), plus one bright star at magnitude 10.3. These numbers imply that we are seeing selection effect behavior, as we discuss more shortly.

One selection effect issue already mentioned is that almost half of our δ Sct star candidates are HADS stars, so we probably are not discovering all of the low amplitude candidates. This would be exacerbated if many of these stars have periods less than 2 hours; the undersampling of the light curve with long-cadence data would reduce the inferred pulsation amplitude. Given the faintness of our stars, low amplitude modes – especially if they are undersampled – may well have their observed amplitudes reduced to below the detection limit of *Kepler*. We also examined the T_{eff} distribution of our target stars, and the bulk of our stars (see Figure 2) lie between 6200 and 7000 K, which is quite a bit cooler than the Uytterhoeven et al. (2011) study, where most stars lie between 6500 and 8400 K and Balona and Dziembowski (2011; 6600 to 8900 K) and Balona et al. (2011; 6300 to 7200 K). The cooler temperature stars in our sample would bias us towards detecting γ Dor stars rather than δ Sct or hybrid stars.

Finally, we examined the possibility that the falloff with magnitude is due to the fainter stars being far enough away to lie between spiral arms in our Galaxy, where we would expect fewer stars. We considered stars with luminosities between $2L_{\odot}$ (cool γ Dor) and $10L_{\odot}$ (hot δ Sct). The distance modulus lies between 10.91 and 12.66 magnitudes (NGC 6791 has a distance modulus of 13.36 mag). Brunthaler et al. (2011) present a schematic map of our Galaxy (see their Figure 2). If we overlay our implied distances (1.5 to 3.4 kpc), they may lie in a space between spiral arms, whereas NGC 6791 (4.7 kpc) lies in the next arm out. Thus, it is possible that the relative numbers of variable stars is being affected by the different sample volumes for the more luminous versus less luminous stars between spiral arms. The γ Dor stars, being less luminous, would be more likely to lie within our spiral arm, where there are more stars. On the other hand the more luminous δ Sct stars in our sample may be far enough away to lie in the interarm space where there are fewer stars. This combination of effects appears to make it less likely to discover faint, low amplitude δ Sct and hybrid stars, and would explain the relative lack of these stars in our sample.

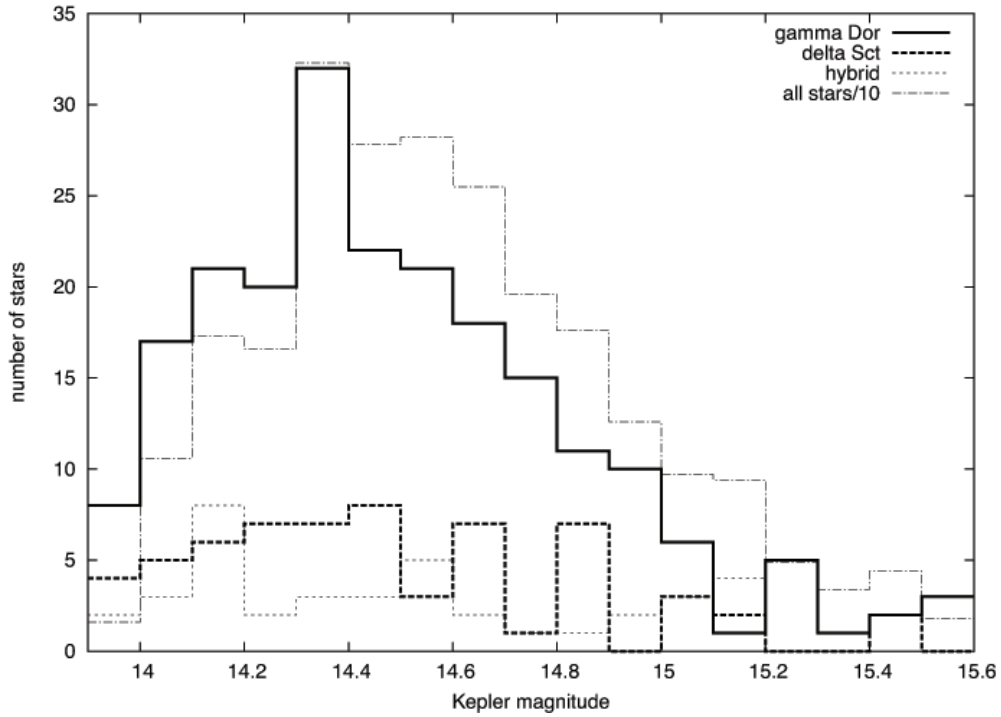


Fig. 10.— Histogram of the γ Dor, δ Sct, and hybrid candidate stars binned by *Kepler* magnitude (K_p). The γ Dor star candidates (solid line) have a distribution that resembles the overall sample (dotted line). The δ Sct star candidates (long-dashed line), and hybrid star candidates (short dashed line) do not have obvious peaks in their distributions, but both have very few stars fainter than K_p magnitude 15.

5. Summary

In this study, we examined the light curves of 2768 stars, mostly between magnitudes 14 and 15, that were selected with temperatures between 6200 and 8200 K, placing them in or near the known γ Dor and δ Sct instability strips. We found 1531 stars that exhibited some sort of variability in their light curves, of which 207 are γ Dor candidate stars, 84 are δ Sct candidate stars, and 32 are hybrid candidate stars. The temperature distribution of our γ Dor, δ Sct, and hybrid stars is similar to that of Balona et al. (2011), Balona & Dziembowski (2011) and Uytterhoeven et al. (2011). Almost all of our γ Dor candidates lie between 6100 and 7500 K, which is similar to the values of Balona et al. (2011), but cooler than that of Uytterhoeven et al. (2011). Our sample has more stars below the red edge of the ground based instability strip ($\sim 50\%$) than the other two studies, which is the result of the effective temperature distribution of our sample. Our hybrid star candidates are scattered nearly uniformly from 6100 to 8000 K, and this is consistent with Uytterhoeven et al. (2011), except that their temperature range is 6600 to 8200 K. Finally, our δ Sct candidate sample has far more cool stars (below about 6700 K) than Balona & Dziembowski (2011) or Uytterhoeven et al. (2011), but if we remove the our HADS candidates (recall that these may well be rotating, spotted stars), then many of our δ Sct candidates lie in or near the ground based δ Sct instability strip. Guzik et al. (2013, 2014) found a few constant (no FT peaks greater than 20 ppm) stars within the ground-based instability strips as well.

We also found 76 binary systems and 1132 stars with low frequency variations that we attribute to rotation or some other phenomenon. We note that nine of the rotating stars have T_{eff} values over 8000K and have properties similar to the ones discussed by Balona (2013). We compared the relative detection rates of γ Dor, δ Sct, and hybrid star candidates and find that our sample is dominated by γ Dor candidates, at 64%. We also note that many of our δ Sct star candidates are HADS stars, which are easier to detect due to their large amplitudes and longer periods than the average δ Sct star. Short cadence data might help detect more δ Sct stars. We found 323 γ Dor, δ Sct, and hybrid stars, but in all three cases the number of discoveries falls off rapidly at a magnitude fainter than 15.0, implying that selection effects are limiting the number of faint stars we can discover. One possibility is that the fainter stars are far enough away to lie between spiral arms in our Galaxy, where there would be fewer stars.

We acknowledge support from the *Kepler* Guest Observer program. Part of this work was funded by NASA grants Cycles 1-4. This paper includes data collected by the *Kepler* mission. Funding for the *Kepler* mission is provided by the NASA Science Mission Directorate.

K.U. acknowledges support from the Spanish National Plan of R&D for 2010, project AYA2010-17803. The research leading to these results has received funding from the European Community's Seventh Framework Programme (FP7/2007-2013) under grant agreement no. 269194. This project benefited from Project FP-7-PEOPLE-IRSES:ASK Np. 269194. We acknowledge fruitful discussions with Andrezj Pigulski, Joanna Molenda-Zakowicz, Patrick Gaulme, and Gerald Handler. We

thank the anonymous referee for their careful reading of the manuscript and comments, which greatly improved this paper.

Facilities: Kepler.

REFERENCES

- Balona, L.A., 2011, MNRAS, 415, 1691
- Balona, L.A., 2012, MNRAS, 423, 3420
- Balona, L.A., 2013, MNRAS, 431, 2240
- Balona, L. A. & Dziembowski, W.A., 2011, MNRAS, 417, 591
- Balona, L.A., Guzik, J.A., Uytterhoeven, K., et al., 2011, MNRAS, 415, 3531
- Borucki, W.J., Koch, D.G., Brown, T.M., et al. 2010, Science, 327, 977
- Bouabid, M.-P., Dupret, M.-A., Salmon, et al., 2013, MNRAS, 429, 2500
- Brown, T.M., Latham, D.W., Everett, M.E., & Esquerdo, G.A., 2011, AJ, 142, 112
- Brunthaler, A., Reid, M.J., Menten, K.M., et al., 2011, Astron. Nachr., 332, 461
- Chapellier, E., Rodriguez, E., Auvergne, M., 2011, A&A, 525, A23
- Cox, A.N., 2000, Allens Astrophysical Quantities, 4th ed, (New York; Springer-Verlag)
- Deeming, T., 1975, ApSS, 36, 137
- Dupret, M.-A., Grigahcène, A., Garrido, R. Gabriel, M., & Scuflaire, R., 2004, A&A, 414, L17
- Garcia Hernandez, A., Moya, A., & Michel, E., 2009, A&A, 506, 79
- Gaulme, P. & Guzik, J.A., 2014, in Proc IAU Symp 301: Precision Asteroseismology, eds. J.A. Guzik, W. Chaplin, G. Handler, & A. Pigulski, (Cambridge; Cambridge U. Press), p 413
- Gilliland R.L. et al., 2010, PASP, 122, 131
- Grigahcène, A., Dupret, M.-A., Garrido, R. Gabriel, M., & Scuflaire, R., 2005, A&A, 434, 1055
- Grigahcène, A., Antoci, V., Balona, L., et al., 2010, ApJ, 713, L192
- Guzik, J.A., Kaye, A.B., Bradley, P.A., Cox, A.N., & Neuforge, C., 2000, ApJ, 542, 57
- Guzik, J.A., Bradley, P.A., Jackiewicz, J., Uytterhoeven, K., & Kinemuchi, K. 2013, Astronomical Review, published online 3 October 2013

- Guzik, J.A., Bradley, P.A., Jackiewicz, J., Uytterhoeven, K., and Kinemuchi, K. 2014, in Proc IAU Symp 301: Precision Asteroseismology, eds. J.A. Guzik, W. Chaplin, G. Handler, and A. Pigulski, (Cambridge; Cambridge U. Press), p 63
- Handler, G., 2009, MNRAS, 398, 1339
- Handler, G., and Shobbrook, R.R., 2002, MNRAS, 333, 251
- Hareter, M., Reegan, P., Miglio, A., et al., 2010, AN, P49 [arXiv1007.3176] (proceedings of the 4th HELAS international conference)
- Henry, G.W., and Feckel, F.C., 2005, AJ, 129, 2026
- Jenkins, J.M. et al., 2010, ApJ, 713, L120
- Kinemuchi, K., Still, M., Fanelli, M., (2011), BAAS, 43, abstract #201.06
- King, H., Matthews, J.M., Rowe, J.F., et al., 2006, CoAst, 148, 28
- Koch, D.J., Borucki, W.J., Basri, G., et al. 2010, ApJ, 713, L79
- McNamara, B.J., Jackiewicz, J., McKeever, J. 2012, AJ, 143, 101
- Molenda-Zakowicz, J., Latham, D.W., Catanzaro, G., et al. 2011, MNRAS, 412, 1210
- Murphy, S.J., Shibahashi, H., and Kurtz, D.W., 2013, MNRAS, 430, 2986
- Pigulski, A., Pojmanski, G., Pilecki, B., and Szczygiel, D., 2010, <http://www.astro.uni.wroc.pl/ldb/asas/Kepler.html>
- Pinsonneault, M.H., An, D., Molenda-Zakowicz, J., Chaplin, W.J., Metcalfe, T.S. & Bruntt, H., 2012, ApJS, 199, 30
- Poretti, E., Michel, E, Garrido, R., et al., 2009, A&A, 506, 85
- Rodriguez, E. and Breger, M. 2001, A&A, 366, 178
- Rowe, J.F., Matthews, J.M., Cameron, C., 2006, CoAst, 148, 34
- Tkachenko, A. Aerts, C., Yakushechkin, A., et al., 2013, *a*, 556, A52
- Thompson, S. E. & Fraquelli, D., 2012, Kepler Archive Manual (KDMC-10008-003), <http://archive.stsci.edu/kepler/documents.html>.
- Thompson, S.E., Everett, M., Mullally, F., et al., 2012, ApJ, 753, 86
- Uytterhoeven, K., Mathias, P., Poretti, E., et al. 2008, A&A, 489, 2213
- Uytterhoeven, K., Moya, A., Grigahcène, A., et al. 2011, A&A, 534, A125

Table 8. γ Dor candidate stars found in our survey

KIC #	K_p	T_{eff}	$\log g$	class	Freq. Range (d^{-1})	Ampl. high (ppm)	Freq. high (d^{-1})
2167444	14.1	7140	4.1	MULT	0.5 – 5.2	1730	0.8082
2448307	14.0	7350	3.9	MULT	0.2 – 3.5	1390	1.2516
2579595	14.1	7150	4.1	ASYM	0.7 – 1.7	5175	1.2205
2581964	14.0	7410	4.2	ASYM	0.4 – 1.5	5914	0.5389
2857178	14.6	7440	4.2	ASYM	0.9 – 2.0	392	1.7313
2974858	14.4	7010	4.2	MULT	0.75 – 3.1	49	2.0287
2975214	14.0	6860	4.2	MULT	0.25 – 0.5	69	0.3131
2985526	14.4	6180	4.3	MULT	.25 – 1.2	53	0.3737
2996232	14.1	7180	4.2	ASYM	0.35 – 1.5	420	0.9369
3248951	14.3	7270	4.3	SYM	0.25 – 3.0	400	1.4643
3556003	14.3	6710	4.1	SYM	0.75 – 1.25	6100	0.9381
3660010	14.2	6360	4.4	SYM	0.35 – 1.0	3500	0.3902
3853742	14.1	7280	4.2	SYM	0.25 – 0.75	335	0.4416
3947031	14.1	7270	4.2	SYM	0.75 – 1.5	432	0.9082
3964570	14.0	6760	4.3	SYM	0.75 – 1.25	1140	1.0841
3966800	14.7	6680	3.9	MULT	0.25 – 1.5	101	0.3294
3967081	14.2	6700	4.2	SYM	0.25 – 2.75	3330	1.2850
4155654	15.4	7360	3.9	MULT	0.20 – 0.75	132	0.2208
4281025	14.0	6300	4.4	MULT	0.20 – 1.0	390	0.4136
4346807	14.9	6480	4.3	SYM	0.35 – 0.75	300	0.4596
4365676	14.5	6450	4.3	SYM	0.5 – 1.4	7350	0.6464
4372107	15.0	7660	4.2	SYM	1.3 – 1.8	3500	1.6250
4554290	14.3	6620	4.4	MULT	0.25 – 1.2	1530	0.3558
4561941	14.6	6550	3.8	MULT	0.25 – 1.0	1390	0.6437
4566563	14.2	7090	4.2	MULT	0.3 – 1.5	250	0.3435
4568058	14.4	7380	4.2	SYM	0.8 – 1.3	8000	1.0794
4568087	14.8	7350	4.1	SYM	0.7 – 1.0	2200	0.8505
4572083	14.9	6880	4.3	SYM	0.8 – 1.2	13000	0.8925
4830647	14.0	7270	4.1	MULT	0.9 – 4.0	1600	1.5175
4840978	14.6	6410	4.3	MULT	0.5 – 1.3	150	0.6250
4841423	14.6	6820	4.1	MULT	0.6 – 1.0	75	0.6529
4843904	14.2	6410	4.3	MULT	0.2 – 0.8	90	0.2967
4930756	15.2	7280	4.3	MULT	0.25 – 1.5	1100	0.3350
4934217	14.2	7560	3.8	ASYM	0.4 – 1.0	7960	0.8809
5097566	14.3	6640	4.3	MULT	0.5 – 1.6	150	0.5071
5108395	14.2	6440	4.4	SYM	0.3 – 1.2	900	0.3929
5113089	14.7	6520	4.4	MULT	0.7 – 2.0	70	0.8333
5120569	14.1	6500	4.0	MULT	0.2 – 1.0	165	0.2310
5123134	14.3	6510	4.4	MULT	0.2 – 3.0	1250	0.4151
5253199	15.3	7300	4.1	ASYM	0.6 – 1.5	13,150	0.6882
5254176	14.7	6880	4.1	ASYM	0.4 – 1.6	15,780	0.7878
5280974	14.4	7010	4.2	SYM	0.75 – 1.75	14,000	1.5210
5281931	15.0	6860	4.2	MULT	0.25 – 1.25	240	0.3551
5342935	14.0	6760	4.4	MULT	0.6 – 2.0	1905	0.6849
5357521	14.8	7490	4.1	MULT	0.5 – 4.0	2100	2.0832

Table 8—Continued

KIC #	K_p	T_{eff}	$\log g$	class	Freq. Range	Ampl. high	Freq. high
5471623	14.1	6770	4.1	MULT	0.2 – 2.2	2300	0.2488
5524370	14.5	7710	4.0	SYM	0.4 – 0.8	6570	0.6143
5529141	14.3	7270	4.2	SYM	1.1 – 2.5	2935	1.6944
5531052	14.2	6850	4.2	MULT	0.5 – 1.0	1950	0.7400
5541405	14.6	6400	4.4	MULT	0.25 – 0.75	220	0.3271
5543818	14.5	6290	4.3	SYM	0.2 – 0.4	1250	0.2033
5561007	14.2	7690	4.2	MULT	1.0 – 6.0	6915	1.2411
5615977	14.9	6820	4.2	SYM	0.25 – 0.7	2440	0.3213
5633114	14.8	7090	4.2	SYM	0.5 – 2.75	750	1.6098
5696153	14.1	7270	4.0	MULT	0.25 – 1.5	2600	0.3022
5717449	14.9	7480	4.1	MULT	0.25 – 4.25	1200	1.8505
5723583	14.7	6460	4.2	MULT	0.3 – 0.7	2010	0.5710
5724633	14.2	6410	3.9	MULT	0.8 – 4.0	2885	2.6317
5869220	14.4	6680	4.2	MULT	0.3 – 0.9	1815	0.4586
5878159	14.6	7330	4.0	ASYM	0.3 – 1.0	13,905	0.3690
5879583	14.3	7400	4.0	ASYM	2.3 – 2.5	67,390	2.3872
5880445	14.3	7390	4.3	MULT	1.1 – 2.6	6280	1.3180
5888202	14.1	6360	4.2	MULT	0.2 – 0.7	400	0.2103
5893541	14.5	6560	4.3	MULT	0.5 – 1.25	2025	0.5944
5899833	14.5	6520	4.0	ASYM	0.4 – 1.25	9800	0.4798
5954775	14.6	6540	4.2	MULT	0.2 – 0.6	3445	0.2962
5954946	14.3	6680	4.3	MULT	0.25 – 1.0	90	0.4369
5957185	14.3	7080	4.1	MULT	0.3 – 1.8	1845	0.6106
5960912	14.7	6840	4.4	MULT	0.5 – 1.0	1525	0.6642
6035618	15.7	7400	4.1	ASYM	0.75 – 1.25	249,840	1.0936
6048208	14.9	6880	4.3	MULT	0.25 – 1.0	1230	0.3151
6119163	14.6	7350	4.0	MULT	1.0 – 3.5	1425	1.1344
6128330	14.0	7450	4.0	ASYM	0.25 – 1.1	21,925	0.4553
6130543	14.7	6840	4.3	MULT	0.25 – 1.0	1690	0.4293
6131093	9.3	6640	4.4	MULT	1.25 – 4.0	17,090	1.5923
6145991	14.1	6210	4.2	MULT	1.0 – 2.0	1615	1.1428
6187850	14.2	6260	4.2	SYM	0.25 – 0.75	930	0.3526
6197138	14.5	6600	4.3	SYM	0.25 – 0.75	2750	0.3575
6210324	14.5	7580	4.0	MULT	0.20 – 5.0	625	2.4603
6220939	14.4	6580	4.5	MULT	0.20 – 1.5	105	0.2336
6230552	14.6	6600	4.3	ASYM	0.75 – 2.0	17,000	1.5467
6279848	8.9	N.A.	N.A.	MULT	0.75 – 1.6	109,900	1.1552
6301965	14.3	7080	4.2	MULT	0.5 – 3.7	225	0.9065
6302177	14.3	6840	4.2	SYM	1.25 – 3.25	175	1.4883
6302332	14.0	6270	4.1	SYM	0.25 – 0.80	2300	0.3435
6302576	14.4	7200	4.1	MULT	0.25 – 3.1	370	1.0724
6302810	14.3	6900	4.1	MULT	0.25 – 1.0	65	0.2804
6305211	14.4	7040	4.2	ASYM	0.25 – 0.75	430	0.4533
6311979	14.5	6150	4.3	ASYM	0.20 – 0.60	2300	0.2617
6370357	14.5	6180	4.3	SYM	0.25 – 0.60	3400	0.2991
6373589	14.2	7250	3.9	MULT	0.25 – 1.25	53	0.3271

Table 8—Continued

KIC #	K_p	T_{eff}	$\log g$	class	Freq. Range	Ampl. high	Freq. high
6373976	14.5	6900	4.3	MULT	0.25 – 1.0	65	0.2804
6388558	14.3	6820	4.1	MULT	0.9 – 4.6	800	3.1682
6497099	14.8	6880	4.2	ASYM	0.25 – 0.9	6650	0.4136
6509590	14.7	7690	4.1	SYM	1.8 – 4.6	725	2.4369
6509962	14.6	6700	4.2	SYM	0.4 – 1.6	425	0.4883
6515882	14.5	7060	4.3	SYM	0.4 – 1.5	11875	1.3214
6521724	14.4	6340	4.3	SYM	0.25 – 0.75	1610	0.3481
6526666	14.2	7030	4.2	SYM	0.3 – 0.8	160	0.5000
6547130	14.1	6460	4.0	ASYM	0.8 – 2.5	15000	1.1869
6580506	14.5	7070	4.0	MULT	0.25 – 2.5	1510	0.5838
6599573	14.4	7290	4.2	MULT	1.0 – 4.3	60	2.1429
6628926	14.1	6220	4.1	SYM	1.3 – 2.5	3200	2.0818
6691019	15.0	6950	4.3	ASYM	1.1 – 3.6	2000	1.2600
6700412	14.8	7430	4.0	SYM	0.5 – 0.8	1475	0.6117
6708546	14.3	6580	4.4	MULT	0.3 – 1.5	75	0.5093
6721297	14.8	6550	4.3	ASYM	0.75 – 1.8	5000	1.7500
6764033	14.0	6920	4.2	SYM	0.2 – 0.4	135	0.2617
6777294	14.5	6640	4.3	SYM	0.25 – 0.6	2250	0.2550
6778212	14.4	7360	4.1	MULT	0.3 – 1.1	35	0.3598
6778479	14.9	7090	4.2	MULT	0.3 – 1.1	55	1.4405
6791943	15.0	6310	4.4	SYM	0.2 – 0.8	2200	0.2500
6803941	14.2	6100	3.7	MULT	0.2 – 0.75	110	0.2804
6870063	14.7	6720	4.3	MULT	0.3 – 1.25	90	0.3621
6871727	14.4	7010	4.2	MULT	0.2 – 0.7	135	0.3435
6878998	14.3	6200	4.3	MULT	0.35 – 2.0	80	0.4136
6937000	14.7	6120	4.3	SYM	0.5 – 1.25	2000	0.6117
6954657	14.7	6860	4.3	MULT	0.25 – 4.0	32	2.0000
6964677	14.2	6760	4.2	MULT	1.5 – 3.5	34	2.8262
6965624	15.2	6560	4.4	MULT	0.9 – 3.4	650	1.9369
7019480	14.6	6220	4.3	SYM	0.3 – 1.1	7200	0.3388
7031347	14.6	6910	4.3	SYM	0.3 – 0.5	160	0.4136
7098418	15.5	7350	4.2	SYM	1.5 – 3.5	2720	1.7500
7187175	14.9	7070	4.1	MULT	0.2 – 1.5	38730	0.2874
7191437	14.3	6900	4.5	SYM	0.5 – 2.5	90	0.6285
7191683	14.5	7660	4.1	SYM	1.0 – 1.5	750	1.3902
7220299	14.6	6300	4.2	SYM	0.25 – 0.6	410	0.2804
7222218	14.6	6160	4.0	SYM	1.0 – 2.3	175	1.1402
7296779	14.6	6420	4.3	MULT	0.2 – 2.5	190	0.5187
7297626	14.7	6320	4.3	MULT	0.25 – 1.25	85	0.2967
7298757	14.3	6110	4.2	MULT	0.25 – 1.5	35	0.2804
7445690	14.8	6950	4.2	MULT	0.4 – 1.4	80	0.4717
7448050	11.8	7390	4.1	ASYM	1.0 – 1.7	611,990	1.1430
7456325	14.3	6540	4.5	SYM	0.25 – 1.0	800	0.2780
7512583	14.4	6380	4.2	SYM	1.7 – 3.5	3600	1.7383
7523217	14.3	7080	4.3	MULT	0.75 – 2.1	100	0.8225
7534444	14.3	6290	4.4	MULT	0.25 – 0.75	80	0.4486

Table 8—Continued

KIC #	K_p	T_{eff}	$\log g$	class	Freq. Range	Ampl. high	Freq. high
7538543	14.9	6870	4.2	SYM	0.2 – 4.8	900	0.3201
7552602	15.0	8080	3.9	SYM	3.25 – 3.6	370	3.5476
7553070	14.7	6410	4.1	SYM	0.45 – 1.7	1510	1.0030
7581111	15.2	6540	4.2	SYM	0.5 – 1.7	2590	0.5234
7685157	14.0	7270	4.3	SYM	0.75 – 1.5	8940	0.8562
7685306	14.3	7900	4.0	MULT	0.75 – 4.0	12,865	0.7874
7687374	14.5	8020	3.9	ASYM	0.4 – 1.0	5540	0.8435
7693255	14.0	6840	4.2	MULT	0.4 – 1.5	150	0.3971
7756660	14.1	7030	4.2	MULT	0.25 – 1.2	140	0.7500
7765798	14.8	7200	3.9	MULT	0.3 – 1.5	68	0.6869
7767565	9.3	N.A.	N.A.	MULT	1.1 – 4.2	30,065	1.4125
7771914	14.1	6800	4.2	SYM	0.65 – 2.7	125	0.6833
7821231	14.0	6690	4.2	MULT	0.25 – 1.1	500	0.3271
7834518	14.5	7080	4.2	MULT	0.75 – 4.25	125	2.0818
7891007	14.1	6420	4.2	MULT	0.25 – 1.6	145	0.3037
7903015	15.0	6680	4.3	MULT	0.25 – 1.75	110	0.4265
7907511	14.7	6170	4.2	SYM	0.75 – 1.75	4100	0.9720
7908851	14.8	7180	4.1	SYM	1.8 – 3.25	2200	2.6869
7968267	14.3	7260	4.2	SYM	0.3 – 1.1	4670	0.4860
7988596	14.1	6490	4.2	SYM	0.4 – 1.2	570	0.5117
8028916	14.1	7060	4.1	ASYM	0.35 – 1.4	26,095	0.6552
8035262	14.3	7290	4.1	SYM	0.75 – 3.0	2075	1.3196
8113557	14.5	6720	4.1	ASYM	1.2 – 1.7	3900	1.3750
8124401	15.2	6310	3.9	ASYM	1.0 – 1.25	11,000	1.1075
8189115	14.3	6270	4.2	MULT	0.7 – 2.0	100	0.7734
8189504	14.5	6580	4.4	SYM	0.75 – 2.1	700	1.0250
8221845	14.4	7470	4.1	SYM	1.9 – 3.3	1250	2.4439
8221986	14.6	7180	4.1	MULT	0.9 – 2.7	1345	1.2349
8222685	8.9	N.A.	N.A.	ASYM	1.1 – 2.1	120,765	1.2218
8309369	14.9	7260	4.0	SYM	3.75 – 4.25	250	3.9952
8313084	14.8	6500	4.4	MULT	0.25 – 1.0	110	0.2804
8323022	14.4	6280	4.2	MULT	0.2 – 2.0	120	0.4416
8327168	14.5	6300	4.3	SYM	0.45 – 1.2	1600	0.5050
8359028	14.4	6740	4.3	SYM	0.35 – 1.0	1100	0.7617
8398162	14.3	6530	4.3	SYM	0.5 – 1.5	200	0.8037
8410612	14.2	6640	4.2	SYM	0.3 – 1.5	600	0.3785
8415383	14.0	7360	4.1	SYM	1.0 – 4.5	410	3.0327
8478472	14.4	7390	4.1	ASYM	1.1 – 2.3	8600	2.1098
8481328	14.7	7120	4.1	SYM	0.5 – 1.2	160	0.6495
8508852	14.5	6760	4.2	SYM	1.0 – 5.0	210	2.6551
8526232	14.1	6770	4.2	SYM	1.0 – 3.3	2100	1.9556
8638619	14.2	7340	4.3	SYM	1.25 – 2.75	2520	2.2220
8767298	14.6	6640	4.5	SYM	0.3 – 1.9	220	0.7874
8804158	14.1	7020	3.9	SYM	0.75 – 2.0	175	0.7967
8814047	14.3	6860	4.3	SYM	0.3 – 1.3	130	0.5888
9012615	15.2	7240	4.3	MULT	1.3 – 3.0	46	1.4439

Table 8—Continued

KIC #	K_p	T_{eff}	$\log g$	class	Freq. Range	Ampl. high	Freq. high
9050484	14.1	6420	4.0	SYM	0.5 – 3.25	130	0.5374
9053846	14.0	6300	4.1	ASYM	0.9 – 1.5	7300	1.3037
9073315	14.6	7320	4.3	SYM	0.7 – 1.6	49,755	0.76601
9113086	14.8	6540	4.1	SYM	0.45 – 1.25	1500	0.5864
9149977	14.4	6900	4.5	SYM	0.4 – 1.4	120	0.5397
9241468	14.5	6190	3.9	SYM	0.35 – 1.75	110	0.5467
9290681	14.3	7360	4.1	SYM	0.6 – 0.8	1500	0.7850
9304984	14.3	6220	4.4	SYM	0.75 – 21	4400	0.8598
9405431	14.3	7000	4.2	SYM	0.25 – 2.1	120	0.3949
9517548	15.4	6990	4.1	SYM	0.5 – 1.9	2235	0.5759
9569705	15.8	7290	4.0	SYM	0.35 – 1.2	81,730	0.5328
9662168	14.2	7170	4.1	ASYM	0.5 – 1.3	3000	0.6355
9715349	14.2	7320	4.1	ASYM	0.8 – 1.8	3960	1.4571
9905540	14.2	7210	4.1	SYM	0.5 – 2.25	1845	1.0864
9910156	14.3	7330	4.2	SYM	1.5 – 5.0	400	3.9836
9962653	10.1	7240	4.3	ASYM	1.4 – 2.5	6000	2.2827
10015325	14.2	6860	4.3	SYM	0.3 – 1.4	220	0.8318
10096798	14.0	6560	4.3	SYM+ROT	1.1 – 1.75	230	1.4743
10683303	6.0	N.A.	N.A.	SYM+ROT	1.25 – 2.5	880	2.2617
10845049	14.4	7450	4.1	SYM	1.0 – 3.0	3345	1.4481
11233133	14.7	7800	4.1	ASYM	1.5 – 3.5	20,000	1.6869
11657064	14.1	7480	4.0	ASYM	0.4 – 0.8	19,200	0.4656
11803734	14.4	6460	4.2	SYM	0.35 – 1.2	198,360	0.3725
11962187	14.0	7160	4.0	ASYM	0.3 – 2.2	9970	1.0178

Note. — “Ampl. high” and “Freq. high” refer to the amplitude and frequency of the highest amplitude mode in the FT. The T_{eff} and $\log g$ values are rounded from the *Kepler* input catalog.